Theoretical Investigation of the Coordination of N_2 Ligands to the Cluster Ni_3

Hristiyan A. Aleksandrov,[†] Georgi N. Vayssilov,*[,†] and Notker Rösch*[,‡]

Faculty of Chemistry, University of Sofia, 1126 Sofia, Bulgaria, and Department Chemie, Technische Universität München, 85747 Garching, Germany

Received: March 10, 2004; In Final Form: May 6, 2004

Various structures of complexes of the cluster Ni_3 with 3 to 12 N_2 ligands were modeled with a gradient-corrected density functional method. The stability of different types of bonding was considered and the most stable structures of $Ni_3(N_2)_x$ complexes ($x = 3-9, 12$) were determined for neutral, cationic, and anionic systems. For the most stable structure of the neutral complex with three and six N_2 ligands, we calculated average ligand binding energies of 116 and 98 kJ/mol, respectively; the binding energy per ligand decreases with increasing number of ligand molecules. For canonical ensembles of mono- and trinuclear complexes with N_2 ligands at varying molar ratio $k = [N_2]:[Ni_3]$, our results suggest that, in agreement with experiment, the complex $Ni_3(N_2)_6$ is among the dominating species at saturation; yet, at sufficiently large molar ratios k, the trinuclear complex with seven ligands, not observed in experiment, also plays an important role in the simulated distributions. It is unclear whether this partial discrepancy in the product distribution originates from complications to simulate the experimental situation or from some aspects of the experimental procedure. Coordination of more than seven N_2 ligands is predicted to lead to a partial or full destruction of the Ni_3 moieties into mononuclear N_2 ligated complexes. The type of bonding of the N_2 ligands (end-on, side-on, hapticity) was found to affect the characteristics of the complexes, e.g. the binding energy, the charge of the Ni_3 moiety, and the activation of the ligands. End-on coordination of N_2 molecules to a Ni atom of the Ni_3 unit entails the most stable type of bonding, whereas side-on coordination causes a stronger elongation of N−N bonds. The ionization potential and the electron affinity of a Ni_3 cluster were calculated to increase after association of ligands.

I. Introduction

Transition metal clusters of nano- and subnanosize dimensions form a very important class of materials with peculiar and, in various cases, unique properties, different from both bulk materials and single atoms.[1−5] Transition metal clusters and their chemical compounds play an increasing role in such diverse areas as nanomaterials, microelectronics, catalysis, etc. Therefore, it is important to know their structures as well as other properties. Various experimental techniques have been developed to prepare and characterize transition metal clusters of specific nuclearity. One can obtain reliable experimental data for ionization potentials and electron affinities of neutral and charged clusters, the photoelectron spectrum, the polarizability, optical properties, magnetic moments, ligand adsorption capacities, etc.[1,4,6−8] However, there is no experimental method for determining directly the structure of a metal cluster because clusters often are produced in gas-phase beams and they are too small (3−50 atoms) for applying diffraction techniques. Instead, an indirect chemical technique has often been applied for structural analysis that relies on the adsorption of probe molecules on metal clusters, e.g. N_2, CO, H_2, H_2O, or NH_3; hence, the interaction of clusters with ligand molecules was intensively investigated.[1,2,9−13] Riley and co-workers[14,15] developed this method and used various types of probe molecules to characterize Ni and Co clusters of three to more than 100 atoms. Due to the assumed chemical inertness of N_2 molecules, most of these studies were performed by adsorption of such ligands.

Alternatively, one can determine a cluster's structure by computational modeling of various geometries.[5,6] In addition to the calculated stability of cluster isomers, one gains further criteria for corroborating the assignment of a structure by comparing computed and experimentally properties, e.g. the ionization potential (IP), the electronic affinity (EA), and the magnetic moment, as well as photoabsorption and photoelectron spectra.[5,6,16−18] With the development of the chemical probe approach, theoretical investigations of ligated metal clusters (with ligands such as N_2, CO, H_2O, and NH_3) became even more important because computational modeling allows one to check to what extent the cluster structure remains unchanged after coordination of ligands. Earlier density functional studies in our group focused on the structure of various symmetric Ni_x clusters ($x = 2-147$) at both local density and gradient-corrected levels.[1,3,6] We also modeled the interaction of CO molecules with such clusters and rationalized how the magnetic moment of metal clusters is quenched by CO ligand molecules.[3,19] The number of unpaired electrons of a cluster is reduced by a change of the effective state of Ni atoms in the surface layer, from $3d^94s^1$ to $3d^{10}4s^0$, due to Pauli repulsion of the occupied 5σ orbital of CO adsorbates and cluster orbitals formed by the superposition of 4s orbitals of surface Ni atoms.[3]

In the present computational study, we focus on complexes of the cluster Ni_3 with N_2 ligands. With their experiments, Parks et al.[15] showed that this cluster can adsorb up to six ligand molecules; they assumed that the triangle of metal atoms does not undergo any significant change toward a linear structure

* Address correspondence to these authors. E-mail: gnv@chem.uni-sofia.bg and roesch@ch.tum.de.
† University of Sofia.
‡ Technische Universität München.

10.1021/jp048923u CCC: $27.50
Published on Web 06/29/2004

after adsorption of the ligands. However, the structure of the ligand shell and the bonding of the ligands to the metal atoms remained unclear, as did reasons why adsorption complexes with more N_2 ligands were not observed. Reuse et al.[20] carried out theoretical investigations of several adsorption complexes $Ni_x(N_2)_y$ ($x = 2-4$), using a density functional (DF) method based on the local density approximation (LDA). They optimized interatomic distances of three structures of $Ni_3(N_2)_3$ and one of $Ni_3(N_2)_6$, all featuring an equilateral triangular Ni_3 cluster; linear (end-on) coordination of N_2 ligands to Ni atoms caused an elongation of the Ni−Ni distance by 10 and 8 pm for complexes with 3 and 6 ligands, respectively. In $Ni_3(N_2)_3$, orientations of the ligands perpendicular to the Ni−Ni bonds or a linear coordination to Ni atoms were found to be most stable.[20] These calculations suggested that the N_2 ligands in the complexes $Ni_3(N_2)_3$ are bound stronger than those in $Ni_3(N_2)_6$ but the adsorption of the ligands did not change the structure of the cluster; the authors concluded that the chemical probe method can provide information on the structure of bare clusters.

In the present theoretical investigation, we estimated the stability of the complexes $Ni_3(N_2)_x$ ($x = 3-9$, 12), as neutral, cationic, and anionic systems, based on DF calculations with a gradient-corrected functional (generalized gradient approximation, GGA). We considered over 50 structures of different symmetry (D_{3h}, C_{3h}, C_{3v}, C_3, C_{2v}, and C_s). We also calculated some properties of the ligated complexes, e.g., ligand binding energies (BE), IP, and EA values, and the charge distribution, and we studied how they change with the structure of the complex. Furthermore, we discuss possible reasons why experiments fail to find complexes with more than six ligands.

The paper is structured as follows. In the next section, we briefly describe our theoretical method as well as the notation of the types of bonding between Ni_3 cluster and N_2 ligands. In Section III, we discuss our calculated results, and in Section IV we analyze the results and compare them with the experimental data and other theoretical results.

II. Method

We carried out DF calculations at the GGA level, using the gradient corrected exchange-correlation functional suggested by Becke (exchange) and Perdew (correlation);[21] the unrestricted Kohn−Sham procedure was applied in all cases. We used the LCGTO-FF-DF method[22] (linear combination of Gaussian-type orbitals fitting the function density functional) as implemented in the parallel DF program PARAGAUSS.[23,24] Employing analytical energy gradients,[25] we automatically optimized the geometry of all model clusters, using the norm and the maximum component of the displacement gradients of the total energy as well as the displacement step size as criteria of convergence for identifying a local minimum. To facilitate the SCF procedure, we imposed suitable symmetry constraints (D_{3h}, C_{3h}, C_{3v}, C_3, C_{2v}, and C_s); thus, these symmetric structures should be considered as model complexes. For complexes with three and six N_2 ligands, we studied all structures of D_{3h}, C_{3h}, and C_{3v} symmetry and one structure of C_3 symmetry that can be converted into each of the former structures. Structures of complexes with other numbers of ligands were constructed by starting from the most stable structures of clusters with fewer ligands (3 or 6, respectively), but preserving high symmetry. To represent the Kohn−Sham orbitals, we used Gaussian-type basis sets, contracted in the following generalized form: (15s11p6d) → [6s5p3d] for Ni and (9s5p2d) → [5s4p2d] for N.[26] The auxiliary basis set used in the LCGTO-FF-DF method to describe the Hartree part of the electron−electron interaction

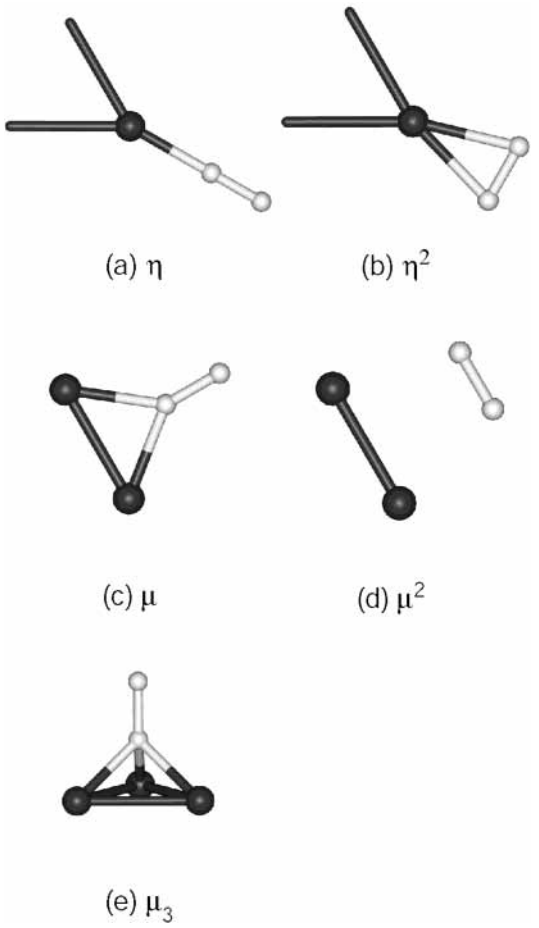

Figure 1. Various types of bonding of N_2 ligands to the Ni_3 moiety: (a) end-on bonding to a Ni atom, η; (b) side-on bonding to a Ni atom, η^2; (c) end-on bonding to a Ni−Ni bond, μ; (d) side-on bonding to a Ni−Ni bond, μ^2; and (e) end-on bonding at a 3-fold position, μ_3.

was derived from the orbital basis set in the usual fashion and augmented by five p-type and five d-type "polarization" exponents for each atom.[22] Vertical IP and EA values of the bare and ligated Ni_3 clusters were estimated with the ΔSCF procedure.

The stability of a complex $Ni_3(N_2)_n$ was evaluated by the average binding energy (BE) per N_2 ligand:

$$\mathrm{BE}[Ni_3(N_2)_n] = -\{E_{tot}[Ni_3(N_2)_n] - E_{tot}(Ni_3) - nE_{tot}(N_2)\}/n$$

The expansion of the nickel cluster due to ligand adsorption was estimated by the differences between Ni−Ni distances in the complex and the corresponding neutral or charged bare Ni_3 cluster. The activation of the ligands was judged by the elongation of the N−N distances in the complex, compared to the calculated bond distance of a neutral N_2 molecule in the gas phase, 110.4 pm, which is slightly larger than the experimental value, 109.75 pm.[27]

To distinguish cluster−ligand isomers of a given composition according to the ligand bonding mode, we use a notation inspired by that common for inorganic complexes. N_2 ligands, coordinated directly to a Ni atom, are denoted by the prefix η (Figure 1a,b), those coordinated to a bond between two metal atoms are denoted by the prefix μ (Figure 1c,d), and those coordinated to three Ni atoms are denoted by the prefix μ_3 (Figure 1e). An upper index describes the number n of atoms of the ligand molecule bound to the cluster: end-on coordination, η and μ (an upper index 1 is omitted for clarity) (Figure 1a,c,e), and

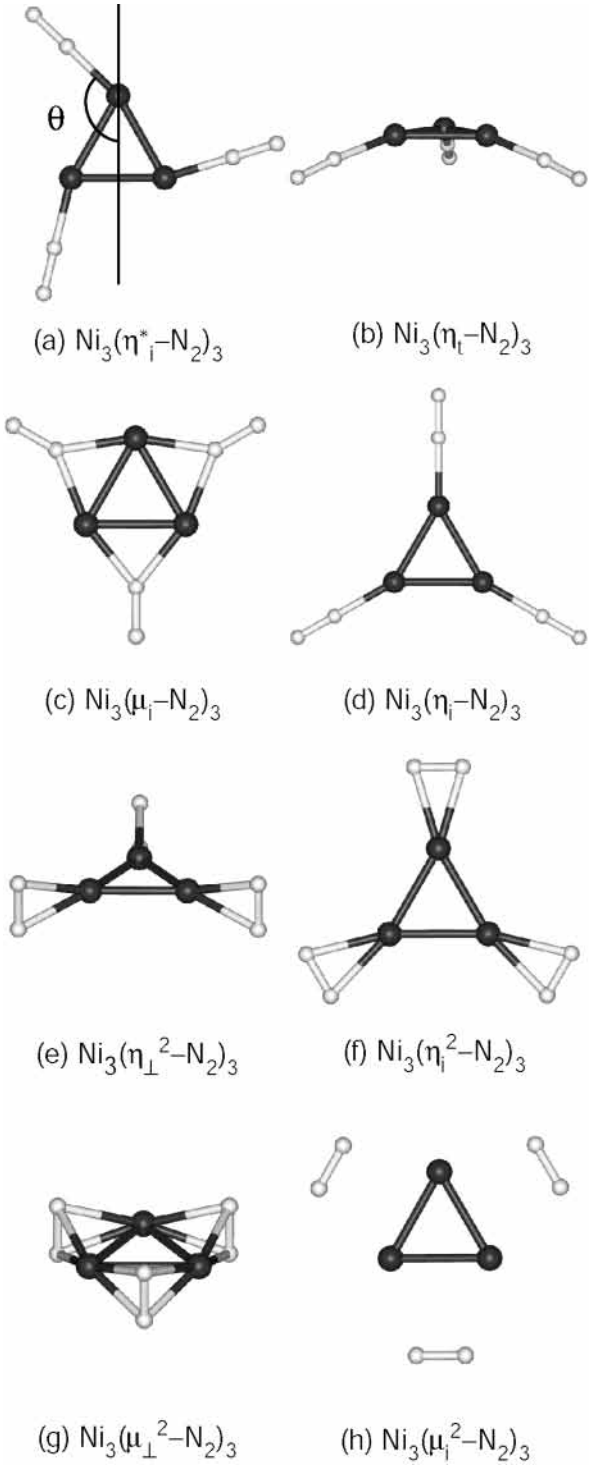

Figure 2. Structures of the Ni_3 moiety with three N_2 ligands. Group I with end-on bonding: (a) $Ni_3(\eta^*_i\text{-}N_2)_3$, (b) $Ni_3(\eta_t\text{-}N_2)_3$, (c) $Ni_3(\mu_i\text{-}N_2)_3$, (d) $Ni_3(\eta_i\text{-}N_2)_3$. Group II with side-on bonding: (e) $Ni_3(\eta^2{}_\perp\text{-}N_2)_3$, (f) $Ni_3(\eta^2{}_i\text{-}N_2)_3$, (g) $Ni_3(\mu^2{}_\perp\text{-}N_2)_3$, (h) $Ni_3(\mu^2{}_i\text{-}N_2)_3$.

side-on coordination, η^2 and μ^2 (Figure 1b,d). Because this notation is ambiguous in several cases, we introduced additional designators. A subscript "i" at a N_2 ligand indicates that it is oriented in the plane of the Ni_3 cluster (Figure 2a,c,d,f,h). If a N_2 ligand is parallel to the plane of the cluster but not in the plane, we denoted it by a subscript "‖" (Figure 4g,h); a subscript "⊥" indicates that N_2 is oriented perpendicular to the cluster plane (Figure 2e,g). Ligands tilted by an angle different from 0° and 90° with respect to the Ni_3 plane are designated by a subscript "t" (Figure 2b). Structures with ligands not located in

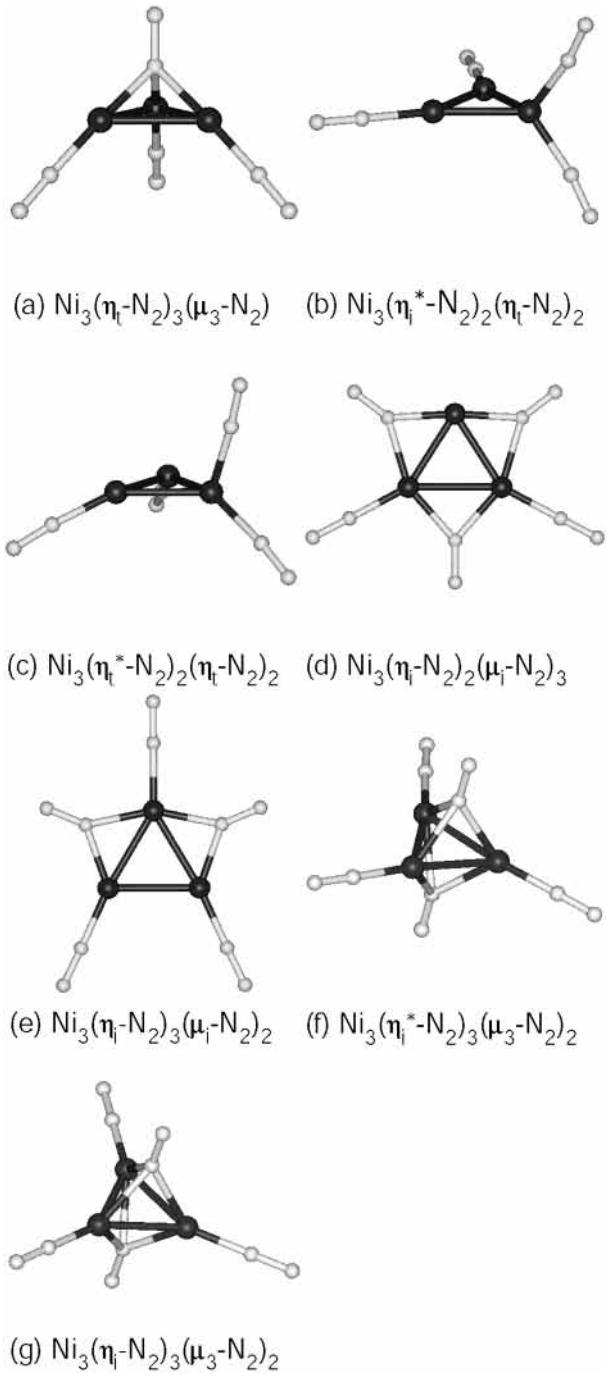

Figure 3. Structures of the Ni_3 moiety with four and five N_2 ligands, $Ni_3(N_2)_4$ and $Ni_3(N_2)_5$: (a) $Ni_3(\eta_t\text{-}N_2)_3(\mu_3\text{-}N_2)$, (b) $Ni_3(\eta^*_i\text{-}N_2)_2(\eta_t\text{-}N_2)_2$, (c) $Ni_3(\eta^*_t\text{-}N_2)_2(\eta_t\text{-}N_2)_2$, (d) $Ni_3(\eta_i\text{-}N_2)_2(\mu_i\text{-}N_2)_3$, (e) $Ni_3(\eta_i\text{-}N_2)_3(\mu_i\text{-}N_2)_2$, (f) $Ni_3(\eta^*_i\text{-}N_2)_3(\mu_3\text{-}N_2)_2$, and (g) $Ni_3(\eta_i\text{-}N_2)_3(\mu_3\text{-}N_2)_2$.

the "vertical" mirror planes of the Ni_3 moiety are designated by an asterisk, $*$ (Figure 2a); in the case of a μ_3* ligand, the asterisk implies that N_2 is not oriented perpendicular to the plane of the Ni_3 moiety (Figure 5a).

In Section III we will discuss various symmetric structures of the complexes $Ni_3(N_2)_x$ ($x = 3-9, 12$) with differently bound ligands. One can easily suggest further structures, especially of lower symmetry. In some selected cases we studied structures with lower symmetry. However, we refrained from further refining all geometries at lower symmetry because the goal of this study cannot be an exhaustive study of all structures. Rather, we intend to present an overview of various possible ways of bonding of N_2 ligands to the nickel cluster and, in the spirit of

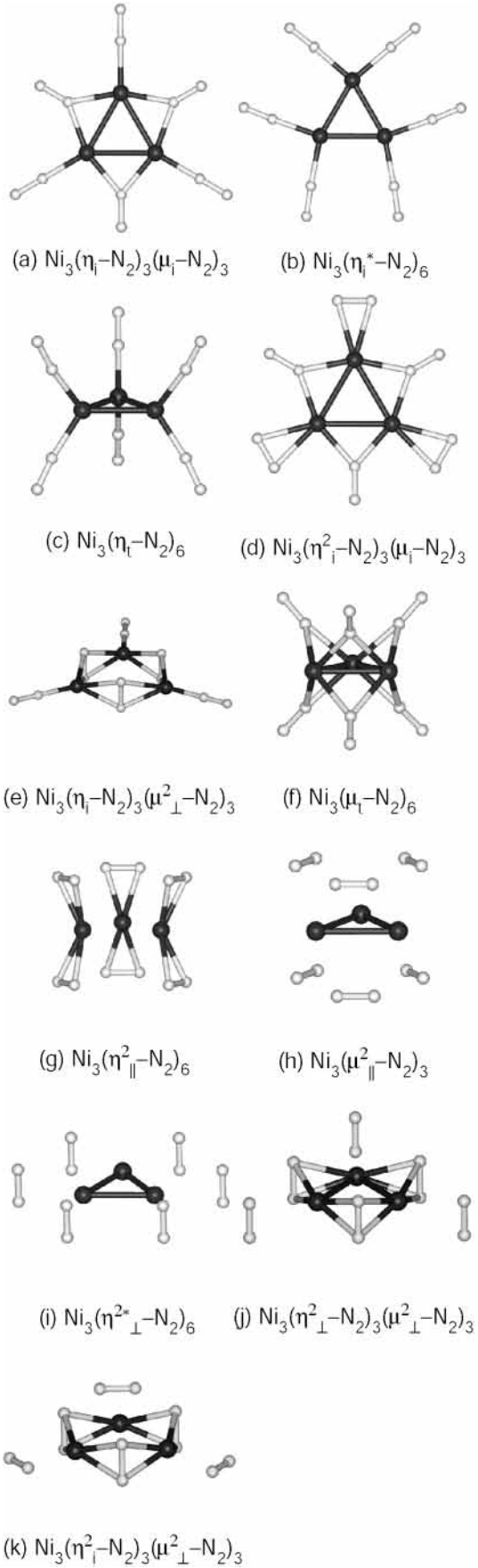

Figure 4. Structures of the Ni_3 moiety with six N_2 ligands: (a) $Ni_3(\eta_i\text{-}N_2)_3(\mu_i\text{-}N_2)_3$, (b) $Ni_3(\eta^*_i\text{-}N_2)_6$, (c) $Ni_3(\eta_t\text{-}N_2)_6$, (d) $Ni_3(\eta^2_i\text{-}N_2)_3(\mu_i\text{-}N_2)_3$, (e) $Ni_3(\eta_i\text{-}N_2)_3(\mu^2{}_\perp\text{-}N_2)_3$, (f) $Ni_3(\mu_t\text{-}N_2)_6$, (g) $Ni_3(\eta^2{}_\parallel\text{-}N_2)_6$, (h) $Ni_3(\mu^2{}_\parallel\text{-}N_2)_6$, (i) $Ni_3(\eta^{2*}{}_\perp\text{-}N_2)_6$, (j) $Ni_3(\eta^2{}_\perp\text{-}N_2)_3(\mu^2{}_\perp\text{-}N_2)_3$, and (k) $Ni_3(\eta^2_i\text{-}N_2)_3(\mu^2{}_\perp\text{-}N_2)_3$.

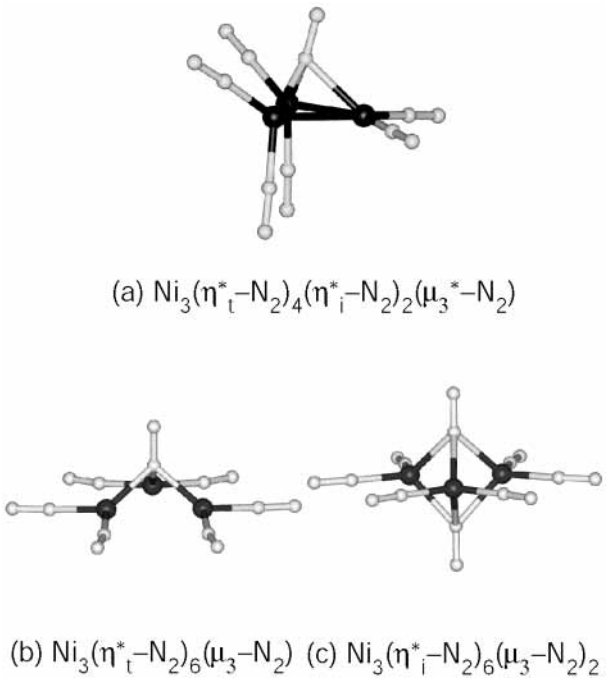

Figure 5. Structures of the Ni_3 moiety with seven and eight N_2 ligands: (a) $Ni_3(\eta^*_t\text{-}N_2)_4(\eta^*_i\text{-}N_2)_2(\mu_3{}^*\text{-}N_2)$, (b) $Ni_3(\eta^*_t\text{-}N_2)_6(\mu_3\text{-}N_2)$, and (c) $Ni_3(\eta^*_i\text{-}N_2)_6(\mu_3\text{-}N_2)_2$.

an extensive model study, we restricted ourselves to symmetric complexes.

The optimized structures and the calculated electronic characteristics of the complexes are summarized in Tables 1 and 2. Properties of cationic and anionic complexes are denoted by superscripts + or −, respectively; for instance, BE^+ designates a BE value obtained for a cationic species. All cationic and anionic structures feature open shells with an odd number of electrons. Therefore, a specific problem arises for those that have extended Ni−Ni or Ni−N bonds because the self-interaction error of common exchange−correlation functionals[28] (e.g. of the GGA used here) can result in erroneous charge delocalization and ultimately in a wrong bond dissociation behavior of a radical when the difference between the IP of one of the final fragments and the EA of another fragment are similar.[29] These conditions hold especially for ionic systems that decompose into equivalent fragments, one of which is charged, so $IP(A^-) = EA(A)$ or $IP(A) = EA(A^+)$. For the systems under study, this condition may occur in ionic structures with extended Ni−Ni bonds that correspond to a decomposition of the central Ni_3 cluster into equivalent fragments; thus, such structures, where observed, were excluded from the discussion. On the other hand, in ionic structures where only N_2 ligands are separated (distant) from the cluster, the self-interaction error does not appear to be important because both the adiabatic IP and EA of the N_2 molecule, 15.41 and −2.34 eV, are far from the values of the remaining $Ni_3(N_2)_n$ complexes (Section IV.C). Note that the self-interaction error is much smaller for neutral close-shell systems,[29] even for structures with extended Ni−Ni bonds or for partially or fully decomposed $Ni_3(N_2)_n$ complexes.

III. Results

A. Ni_3 Cluster. Previous calculations showed that the cluster Ni_3 forms essentially an equilateral triangle with a Ni−Ni distance between 215 and 224 pm, depending on the employed computational approach (see Section IV.D).[30] As an initial step in our study, we also optimized the structure of bare Ni_3 with

TABLE 1: Interatomic Distances (pm) of the Complexes $Ni_3(N_2)_x$ ($x = 3-9$) in Neutral, Cationic, and Anionic Form: Expansion Δ(Ni−Ni) of the Ni_3 Cluster; Elongation Δ(N−N) of the N−N Bond in N_2 Ligands; and Length R(Ni−N) of the Ni−N Bonds for Linear Bonding Ligands[a]

	Δ(Ni−Ni)			R(Ni−N)			R(Ni−N)^{br}			Δ(N−N)			Δ(N−N)^{br}		
	−1	0	+1	−1	0	+1	−1	0	+1	−1	0	+1	−1	0	+1
$Ni_3(\eta^*_i\text{-}N_2)_3$	5	3	1	175	175	182				3.4	2.1	0.8			
$Ni_3(\eta_t\text{-}N_2)_3$	6	5	3	176	182	191				3.1	1.6	0.4			
$Ni_3(\mu_i\text{-}N_2)_3$	5	6	8				188	187	191				6.3	4.8	3.3
$Ni_3(\eta_i\text{-}N_2)_3$	6	8	5	176	182	190				3.1	1.6	0.5			
$Ni_3(\eta^2_\perp\text{-}N_2)_3$	6	0	1	193	199	218				6.0	4.2	1.6			
$Ni_3(\eta^2_i\text{-}N_2)_3$	8	8	1	197	202	217				5.1	3.7	1.7			
$Ni_3(\mu^2_\perp\text{-}N_2)_3$ (1)[b]	33	60[c]					197	197					12.0	9.5	
$Ni_3(\mu^2_\perp\text{-}N_2)_3$ (2)[b]	7	18	21				203	203	204				10.6	7.7	6.3
$Ni_3(\mu^2_i\text{-}N_2)_3$	0	3	−1				286	229	304				1.8	2.7	0.0
$Ni_3(\eta_t\text{-}N_2)_3(\mu_3\text{-}N_2)$	23	22	14	174	178	184	186[d]	184[d]	187[d]	3.2	1.8	0.7	11.4[d]	8.5[d]	6.9[d]
$Ni_3(\eta^*_t\text{-}N_2)_2(\eta_t\text{-}N_2)_2$	3	2	−2	178−	180−	190−				2.9−	1.3−	0.5−			
	15	11	12	179	188	196				3.0	1.8	0.7			
$Ni_3(\eta^*_i\text{-}N_2)_2(\eta_t\text{-}N_2)_2$	3	1	−3	179	188	192				2.9	1.2	0.6			
	16	11	16	178	181	191				3.0	1.8	0.5			
$Ni_3(\eta_i\text{-}N_2)_2(\mu_i\text{-}N_2)_3$[e]	9	10	29	178	182	188	187	183−	187−	3.2	1.5	0.6	5.0	3.7	3.0
	26	28	7	176				196	196	2.9				4.1	3.1
$Ni_3(\eta_i\text{-}N_2)_3(\mu_i\text{-}N_2)_2$	15	18	22	182	185	190	184−	183−	184−	2.5	1.2	0.5	5.7	4.2	3.3
	18	22	12	176	179	183	187	189	192	3.1	1.8	0.9			
$Ni_3(\eta^*_i\text{-}N_2)_3(\mu_3\text{-}N_2)_2$	16	11	8	176	178	183	201[d]	203[d]	207[d]	3.3	1.8	0.8	5.9[d]	4.3[d]	3.3[d]
$Ni_3(\eta_i\text{-}N_2)_3(\mu_3\text{-}N_2)_2$	16	10	8	176	178	183	201[d]	203[d]	207[d]	3.3	1.8	0.8	5.9[d]	4.3[d]	3.3[d]
$Ni_3(\eta_i\text{-}N_2)_3(\mu_i\text{-}N_2)_3$	15	19	17	181	184	190	191	191	193	2.4	1.3	0.5	4.9	3.8	3.0
$Ni_3(\eta^*_i\text{-}N_2)_6$	19	8	13	182	184	185				2.4	1.4	0.9			
$Ni_3(\eta_t\text{-}N_2)_6$	30	9	13	176	187	188				2.8	1.3	0.7			
$Ni_3(\eta^2_i\text{-}N_2)_3(\mu_i\text{-}N_2)_3$	24	26	19	207	210	226	192	192	194	3.3	2.6	1.2	5.2	3.4	2.8
$Ni_3(\eta_i\text{-}N_2)_3(\mu^2_\perp\text{-}N_2)_3$	138[c]	138[c]	125[c]	178	182	189	207	206	205	3.1	1.8	0.7	7.9	6.6	6.5
$Ni_3(\mu_t\text{-}N_2)_6$	11	11	12				206	207	210				4.1	3.1	2.1
$Ni_3(\eta^2_{||}\text{-}N_2)_6$	43[c]	40[c]	0	199	199	245				5.1	4.0	0.6			
$Ni_3(\mu^2_{||}\text{-}N_2)_6$	24	24	27				222	222	223				2.8	1.8	1.1
$Ni_3(\eta^{2*}_\perp\text{-}N_2)_6$	10	4	1	233	235	259				1.6	0.9	0.4			
$Ni_3(\eta^2_i\text{-}N_2)_3(\mu^2_\perp\text{-}N_2)_3$	34	63[c]	4	384	335	217	197	197	400	0.0	0.0	1.6	11.9	9.6	0.0
$Ni_3(\eta^2_\perp\text{-}N_2)_3(\mu^2_\perp\text{-}N_2)_3$	17	18	24	219	356	265	214	203	206	3.3	0.0	0.3	7.1	7.7	6.1
$Ni_3(\eta^*_t\text{-}N_2)_4(\eta^*_i\text{-}N_2)_2(\mu_3\text{*-}N_2)$[f]	35	21	15	178−	182−	185−	196	195[d]	190[d]	2.5−	1.4−	0.5−	3.8	5.6[d]	4.3[d]
	29	29	25	181	185	193		205[d]	243[d]	2.8	1.7	0.9			
$Ni_3(\eta^*_t\text{-}N_2)_6(\mu_3\text{−}N_2)$	41[d]	53[d]	24	181	183	188	198[d]	194[d]	194[d]	2.6	1.6	0.7	5.7[d]	6.3[d]	5.1[d]
$Ni_3(\eta^*_i\text{-}N_2)_6(\mu_3\text{−}N_2)_2$	42[d]	43[d]	21	182	184	189	211[d]	209[d]	208[d]	2.5	1.5	0.7	5.1[d]	3.9[d]	3.2[d]
$Ni_3(\eta_t\text{-}N_2)_6(\mu_i\text{-}N_2)_3$	51[c]	41[c]	28	185	189	197	198	196	196	2.0	1.2	0.5	4.6	3.1	2.7
$Ni_3(\eta_t\text{-}N_2)_6(\mu^2_\perp\text{-}N_2)_3$	1500[c]	168[c]	158[c]	175	185	190	>900	217	215	2.8	1.3	0.6	−0.2	5.4	5.5
$Ni_3(\eta^2_{||}\text{-}N_2)_6(\mu^2_\perp\text{-}N_2)_3$	166[c]	151[c]	133[c]	219	223	236	214	210	206	2.3	1.5	0.8	7.3	6.2	6.7

[a] Values R(Ni−N)^{br} and Δ(N−N)^{br} for bridge-bound N_2 ligands are shown in separate columns. [b] Two local minima (1) and (2) with similar BE of the neutral and anionic complexes were found for this structure. [c] The Ni_3 moieties in these structures can be considered as decomposed into atomic Ni species. [d] N_2 ligands coordinated end-on at a 3-fold position of the Ni_3 moiety. [e] The optimized anionic structure is $Ni_3(\eta_i\text{-}N_2)_4(\mu_i\text{-}N_2)^-$. [f] The optimized anionic structure is $Ni_3(\eta^*_t\text{-}N_2)_4(\eta^*_i\text{-}N_2)_2(\mu_i\text{-}N_2)^-$.

different symmetry constraints (D_{3h} and C_{2v}) and a fixed number of unpaired electrons, $N_s = 0-8$. The most stable structures feature two unpaired electrons with very similar BE values per Ni atom,[31] 174−175 kJ/mol. Two electronic configurations are almost degenerate, exhibiting similar geometries. In D_{3h} symmetry, there are two such stable configurations with a BE per Ni atom of 175 kJ/mol: $(a_1')^{16}(a_2')^5(e')^{40}(a_1'')^1(a_2'')^6(e'')^{16}$ with R(Ni−Ni) = 223.2 pm and $(a_1')^{16}(a_2')^5(e')^{39}(a_1'')^2(a_2'')^6(e'')^{16}$ with R(Ni−Ni) = 225.6 pm. The electronic configuration $(a_1)^{36}(a_2)^9(b_1)^{14}(b_2)^{25}$ in C_{2v} corresponds to the former configuration in D_{3h} symmetry;[32] it features the same BE per Ni atom, 175 kJ/mol, and a similar geometry:[33] the R(Ni−Ni) distances are 224.5 and 225.7 pm and the apex angle Ni−Ni−Ni is 60.4°. Hence the two structures can be considered as equivalent. These structure differences also characterize the inherent accuracy of the computational strategy. We also considered other configurations, imposing a fixed number $N_s = 0$, 4, 6, or 8 of unpaired electrons. Each manifold of spin−orbitals separately obeys the aufbau principle;[28] however, due to the imposed restriction of the number of unpaired electrons in the cluster, some orbitals of minority spin below the highest occupied molecular orbital (HOMO) of majority spin remained unoccupied. The calculated BE values were also lower, thus these configurations approximate excited states of Ni_3.

The vertical and adiabatic IP values of the optimized cluster in D_{3h} symmetry are 6.48 and 6.29 eV, respectively; the corresponding EA values are 1.05 and 1.28 eV (Table 3).[34] In the cationic (quartet) and anionic (sextet) Ni_3 clusters at D_{3h} symmetry, the Ni−Ni distance increases to 226.5 and 231.1 pm, respectively. In C_{2v} symmetry, the Ni_3 cluster optimized as either cationic or anionic system features (unique) Ni−Ni−Ni angles of 61.4° or 58.2°, respectively; these slight distortions, compared to the D_{3h} constrained results, should be typical for the effect of charge localization.

B. Structure of $Ni_3(N_2)_3$ Complexes. We modeled nine structures of the complex of Ni_3 with three N_2 molecules: six of D_{3h} symmetry as well as structures of C_{3h}, C_{3v}, and C_3 symmetry (Tables 1 and 2). The resulting structures can be divided into two groups. Group I consists of structures in which one of the nitrogen atoms of each ligand is directly coordinated

TABLE 2: Binding Energies BE[a] (kJ/mol) of $Ni_3(N_2)_x$ Complexes ($x = 3-9$) and Charge Distributions (e) of the Neutral Complexes: Charge $Q(Ni_3)$ of the Ni_3 Moiety; Charge Q(N1) of the N Atom Directly Bound to the Ni_3 Unit; Charge Q(N2) of the N Not Directly Bound to the Ni_3 Unit[a,b]

	BE^-	BE	BE^+	$q(Ni_3)$	q(N1)	q(N2)	$q(N1)^{br}$	$q(N2)^{br}$	N_s[c]	symm
$Ni_3(\eta^*_i\text{-}N_2)_3$	142	116	82	0.12	−0.04	0.00			0	C_{3h}
$Ni_3(\eta_t\text{-}N_2)_3$	146	105	86	0.12	−0.06	0.02			2	C_{3v}
$Ni_3(\mu_i\text{-}N_2)_3$	99	102	71	0.72			−0.17	−0.07	0	D_{3h}
$Ni_3(\eta_i\text{-}N_2)_3$	146	100	81	0.18	−0.06	0.00			2	D_{3h}
$Ni_3(\eta^2_\perp\text{-}N_2)_3$	112	65	36	0.39	−0.07				0	D_{3h}
$Ni_3(\eta^2_i\text{-}N_2)_3$	86	63	22	0.30	−0.05				2	D_{3h}
$Ni_3(\mu^2_\perp\text{-}N_2)_3$ (1)[d]	53	42	13	1.21			−0.20		0	D_{3h}
$Ni_3(\mu^2_\perp\text{-}N_2)_3$ (2)[d]	44	41		0.84			−0.14		0	
$Ni_3(\mu^2_i\text{-}N_2)_3$		6	10	0.15			−0.03		2	D_{3h}
$Ni_3(\eta_t\text{-}N_2)_3(\mu_3\text{-}N_2)$	117	107	87	0.54	−0.05	−0.01	−0.31	−0.12	0	C_{3v}
$Ni_3(\eta^*_t\text{-}N_2)_2(\eta_t\text{-}N_2)_2$	123	90	77	0.13	−0.03	0.01			0	C_s
					−0.06	0.02				
$Ni_3(\eta^*_i\text{-}N_2)_2(\eta_t\text{-}N_2)_2$	123	88	74	0.11	−0.05	0.01			0	C_{2v}
					−0.04	0.03				
$Ni_3(\eta_i\text{-}N_2)_2(\mu_i\text{-}N_2)_3$	111[e]	102	78	0.62	−0.01	0.01	−0.15	−0.05	0	C_{2v}
							−0.16	−0.05		
$Ni_3(\eta_i\text{-}N_2)_3(\mu_i\text{-}N_2)_2$	107	101	86	0.47	−0.01	0.03	−0.16	−0.06	0	C_{2v}
					−0.04	0.01				
$Ni_3(\eta^*_i\text{-}N_2)_3(\mu_3\text{-}N_2)_2$	96	89	68	0.53	−0.04	0.00	−0.17	−0.03	0	C_{3h}
$Ni_3(\eta_i\text{-}N_2)_3(\mu_3\text{-}N_2)_2$	96	88	60	0.54	−0.05	0.01	−0.17	−0.03	0	D_{3h}
$Ni_3(\eta_i\text{-}N_2)_3(\mu_i\text{-}N_2)_3$	108	98	78	0.59	−0.01	0.02	−0.15	−0.05	0	D_{3h}
$Ni_3(\eta^*_i\text{-}N_2)_6$	100	84	66	0.06	−0.03	0.02			0	D_{3h}
$Ni_3(\eta_t\text{-}N_2)_6$	108	79	65	0.18	−0.04	0.01			2	D_{3h}
$Ni_3(\eta^2_{||}\text{-}N_2)_3(\mu_i\text{-}N_2)_3$	63	64	46	0.66	−0.02		−0.16	−0.03	0	D_{3h}
$Ni_3(\eta_i\text{-}N_2)_3(\mu^2_\perp\text{-}N_2)_3$	63	53	37	0.86	−0.05	0.01	−0.13		0	D_{3h}
$Ni_3(\mu_t\text{-}N_2)_6$	40	34	24	0.57			−0.08	−0.02	0	D_{3h}
$Ni_3(\eta^2_{||}\text{-}N_2)_6$	37	29	16	0.63	−0.05				0	D_{3h}
$Ni_3(\mu^2_{||}\text{-}N_2)_6$	30	28	17	0.42			−0.04		0	D_{3h}
$Ni_3(\eta^{2*}_\perp\text{-}N_2)_6$	36	23	16	−0.15	0.01				0	D_{3h}
$Ni_3(\eta^2_i\text{-}N_2)_3(\mu^2_\perp\text{-}N_2)_3$	28	22	14	1.14	0.02		−0.21		0	D_{3h}
$Ni_3(\eta^2_\perp\text{-}N_2)_3(\mu^2_\perp\text{-}N_2)_3$	28	21	12	0.75	0.02		−0.14		0	D_{3h}
$Ni_3(\eta^*_t\text{-}N_2)_4(\eta^*_i\text{-}N_2)_2(\mu_3{}^*\text{-}N_2)$	97[f]	87	77	0.42	−0.02	0.01	−0.24	−0.08	0	C_s
					−0.03	0.02				
$Ni_3(\eta^*_t\text{-}N_2)_6(\mu_3\text{-}N_2)$	86	78	73	0.54	−0.04	0.01	−0.30	−0.06	0	C_{3v}
$Ni_3(\eta^*_i\text{-}N_2)_6(\mu_3\text{-}N_2)_2$	76	73	69	0.43	−0.03	0.01	−0.14	−0.02	0	D_{3h}
$Ni_3(\eta_t\text{-}N_2)_6(\mu_i\text{-}N_2)_3$	75	72	63	0.45	−0.02	0.01	−0.11	−0.03	0	D_{3h}
$Ni_3(\eta_t\text{-}N_2)_6(\mu^2_\perp\text{-}N_2)_3$	58	58	46	0.45	−0.01	0.02	−0.09		0	D_{3h}
$Ni_3(\eta^2_{||}\text{-}N_2)_6(\mu^2_\perp\text{-}N_2)_3$	21	24	12	0.63	0.00		−0.11		0	D_{3h}

[a] Values $q(N1)^{br}$ and $q(N2)^{br}$ for bridge-bound N_2 ligands are shown in separate columns. Also shown are the number N_s of unpaired electrons and the symmetry of the complex. [b] The superscripts + and − indicate values of cation and anionic structures, respectively. [c] All singlets exhibit a closed-shell electronic configuration. [d] Values for each local minimum (1) and (2), see Table 1. [e] The optimized anionic structure is $Ni_3(\eta_i\text{-}N_2)_4(\mu_i\text{-}N_2)^-$. [f] The optimized anionic structure is $Ni_3(\eta^*_t\text{-}N_2)_4(\eta^*_i\text{-}N_2)_2(\mu_i\text{-}N_2)^-$.

to the cluster (end-on bonding): $Ni_3(\eta^*_i\text{-}N_2)_3$, $Ni_3(\eta_t\text{-}N_2)_3$, $Ni_3(\eta_i\text{-}N_2)_3$, and $Ni_3(\mu_i\text{-}N_2)_3$ (Figure 2, parts a−d, respectively). In the former two structures, the characteristic angle θ (i.e. the angle between a N atom, the Ni atom the ligand is coordinated to, and the center of the Ni_3 cluster; see Figure 2a) is 133.4° and 171.3°, respectively. Group II comprises structures in which both nitrogen atoms of each ligand molecule are bound to the cluster (side-on bonding): $Ni_3(\eta^2_\perp\text{-}N_2)_3$, $Ni_3(\eta^2_i\text{-}N_2)_3$, $Ni_3(\mu^2_\perp\text{-}N_2)_3$, and $Ni_3(\mu^2_i\text{-}N_2)_3$ (Figure 2, parts e−h, respectively). Because of the small BE value, 6 kJ/mol, the last structure will not be discussed further.

The characteristics of the two groups clearly differ. The BE values of N_2 molecules in structures of Group I, 100−116 kJ/mol, are significantly larger than those of Group II, 42−65 kJ/mol (Table 2). Four of the structures considered exhibit two unpaired electrons whereas the other structures have closed shells, but the spin multiplicity does not correlate with the stability of the structures (Table 2).

In three structures of Group I, $Ni_3(\eta^*_i\text{-}N_2)_3$, $Ni_3(\eta_t\text{-}N_2)_3$, and $Ni_3(\eta_i\text{-}N_2)_3$, N_2 ligands are coordinated to one Ni center and, in the fourth structure, $Ni_3(\mu_i\text{-}N_2)_3$, N_2 ligands are bound to a Ni−Ni bond in a bridge position. Some characteristics of the latter structure are intermediate between those of Groups I and II. The end-on bonded structures exhibit short Ni−N distances, 175−187 pm, whereas in the side-on bonded complexes the Ni−N distances are much longer, 197−202 pm (Table 1). This tendency persists in the corresponding cationic and anionic structures. Group I structures with N_2 bound to a Ni atom show slightly extended N−N bonds, $\Delta(N-N) = 1.6-2.1$ pm, whereas in Group II the extension is larger, 3.7−9.5 pm. For all structures, intraligand N−N bonds are most activated in anionic clusters and least activated in the cations (Table 1): $\Delta(N-N)^- > \Delta(N-N) > \Delta(N-N)^+$.

N_2 ligands of structures of Group I are polarized whereas for ligands of Group II structures this is not possible for symmetry reasons (Table 2). The charges of the Ni_3 moiety of Group I structures with linear bonding of N_2 ligands are much smaller, $q(Ni_3) = 0.12-0.18$ e, compared to those of all other structures, $q(Ni_3) = 0.30-1.21$ e, which include $Ni_3(\mu_i\text{-}N_2)_3$ and Group II. For the structure $Ni_3(\mu^2_\perp\text{-}N_2)_3$ we found two local minima with essentially equal BE, 42 and 41 kJ/mol; they feature a significant expansion of the Ni_3 cluster, $\Delta(Ni-Ni) =$ 60 and 18 pm, respectively, and a strong activation of the N_2 ligands, $\Delta(N-N)^{br} = 9.5$ and 7.7 pm. The Ni−N distance,

TABLE 3: Vertical Ionization Potentials, IP^0, and Electron Affinities, EA^0 (V), of the Neutral Systems, IP^-, of the Corresponding Anionic Systems, EA^+, of Corresponding Cationic Structures as Well as Adiabatic Values IP[a] and EA[a], and the HOMO-LUMO gap ΔE of the Neutral Systems

N[b]	structure	IP^0	IP[a]	EA^0	EA[a]	EA^+	IP^-	ΔE
0	Ni_3 (D_{3h})	6.48	6.29	1.05	1.28	6.28	1.34	0.45
3	$Ni_3(\eta^*_i\text{-}N_2)_3$	7.66	7.34	1.79	2.13	7.22	2.47	0.87
3	$Ni_3(\eta_t\text{-}N_2)_3$	7.30	6.88	2.44	2.58	6.68	2.78	0.32
3	$Ni_3(\mu_i\text{-}N_2)_3$	7.24	7.23	1.19	1.22	7.15	1.26	1.30
3	$Ni_3(\eta_i\text{-}N_2)_3$	7.19	6.85	2.57	2.75	6.75	2.85	0.32
3	$Ni_3(\eta^2_\perp\text{-}N_2)_3$	7.55	7.18	2.66	2.79	6.78	2.66	0.29
3	$Ni_3(\eta^2_i\text{-}N_2)_3$	7.61	7.53	2.03	2.04	7.26	2.09	0.58
3	$Ni_3(\mu^2_\perp\text{-}N_2)_3$	7.50[c]	7.15[c]	1.44[c]	1.67[c]	7.11[c]	1.85[c]	0.88[c]
4	$Ni_3(\eta_t\text{-}N_2)_3(\mu_3\text{-}N_2)$	7.23	7.09	1.61	1.72	6.94	1.83	1.09
4	$Ni_3(\eta^*_t\text{-}N_2)_2(\eta_t\text{-}N_2)_2$	7.02	6.83	2.26	2.69	6.60	2.93	0.57
4	$Ni_3(\eta^*_i\text{-}N_2)_2(\eta_t\text{-}N_2)_2$	7.05	6.88	2.45	2.76	6.65	2.92	0.45
5	$Ni_3(\eta_i\text{-}N_2)_2(\mu_i\text{-}N_2)_3$	7.58	7.50	1.65	1.86	7.41	2.52	1.51
5	$Ni_3(\eta_i\text{-}N_2)_3(\mu_i\text{-}N_2)_2$	7.42	7.06	1.70	1.78	6.81	1.85	1.40
5	$Ni_3(\eta^*_i\text{-}N_2)_3(\mu_3\text{-}N_2)_2$	7.57	7.32	1.53	1.72	7.09	1.88	1.78
5	$Ni_3(\eta_i\text{-}N_2)_3(\mu_3\text{-}N_2)_2$	7.86	7.71	1.63	1.75	7.60	1.88	1.82
6	$Ni_3(\eta_i\text{-}N_2)_3(\mu_i\text{-}N_2)_3$	7.58	7.50	1.84	1.90	7.42	1.96	1.65
6	$Ni_3(\eta^*_i\text{-}N_2)_6$	7.54	7.45	2.12	2.28	7.34	2.48	1.14
6	$Ni_3(\eta_t\text{-}N_2)_6$	7.28	7.16	1.97	3.09	7.01	2.34	1.10
6	$Ni_3(\eta^2_i\text{-}N_2)_3(\mu_i\text{-}N_2)_3$	7.52	7.38	1.20	1.27	7.23	1.33	1.87
6	$Ni_3(\eta_i\text{-}N_2)_3(\mu^2_\perp\text{-}N_2)_3$	7.36	7.24	1.84	1.92	7.12	2.00	1.30
6	$Ni_3(\mu_t\text{-}N_2)_6$	6.95	6.87	1.68	1.73	6.79	1.77	1.05
6	$Ni_3(\eta^2_\parallel\text{-}N_2)_6$	7.31	7.09	1.82	1.87	6.63	1.91	1.04
6	$Ni_3(\mu^2_\parallel\text{-}N_2)_6$	7.05	7.00	1.40	1.44	6.95	1.48	1.20
6	$Ni_3(\eta^{2*}_\perp\text{-}N_2)_6$	7.22	6.68	2.05	2.12	6.30	2.44	0.63
7	$Ni_3(\eta^*_t\text{-}N_2)_4(\eta^*_i\text{-}N_2)_2(\mu_3{}^*\text{-}N_2)$	7.33	7.02	1.73	2.08	6.73	2.46	1.57
7	$Ni_3(\eta^*_t\text{-}N_2)_6(\mu_3\text{-}N_2)$	6.99	6.64	1.72	1.86	6.36	2.01	1.36
8	$Ni_3(\eta^*_i\text{-}N_2)_6(\mu_3\text{-}N_2)_2$	6.87	6.60	1.41	1.49	6.35	1.57	1.54
9	$Ni_3(\eta_t\text{-}N_2)_6(\mu_i\text{-}N_2)_3$	7.41	7.13	1.52	1.64	6.92	1.74	2.01
9	$Ni_3(\eta_t\text{-}N_2)_6(\mu^2_\perp\text{-}N_2)_3$	7.48	7.38	1.22		7.28		2.26

[a] Adiabatic values. [b] Number of ligands of the complex. [c] The corresponding values are for the more stable minimum (1), see Table 1.

$R(Ni{-}N)^{br} = 197$ pm, of the latter, more stable structure is shorter; in the other structure, this bond is $R(Ni{-}N)^{br} = 203$ pm. We also located two minima for the corresponding anionic system, but their energy difference is larger, $BE^- = 53$ and 44 kJ/mol, with elongations $\Delta(Ni{-}Ni)^- = 33$ and 7 pm, respectively. Starting the optimization of the cationic complex from either structure of the neutral cluster yields the same local minimum; with a small value of $\Delta(Ni{-}Ni)^+ = 21$ pm, it resembles the less stable neutral structure.

The most stable neutral structure is $Ni_3(\eta^*_i\text{-}N_2)_3$, BE = 116 kJ/mol, and its stability in the cationic and anionic forms is close to those of the most stable charged structures. The angle θ is 133.4°; in the cationic system, the angle remains essentially unchanged, 134.8°, but it increases to 147.3° in the corresponding anionic system. The most stable cationic structure is $Ni_3(\eta_t\text{-}N_2)_3$ ($BE^+ = 86$ kJ/mol); in anionic form, the most stable structure is $Ni_3(\eta_i\text{-}N_2)_3$ ($BE^- = 146$ kJ/mol). One might have anticipated that, as anionic systems, the structures $Ni_3(\eta^*_i\text{-}N_2)_3$ and $Ni_3(\eta_t\text{-}N_2)_3$ transform during geometry optimization into $Ni_3(\eta_i\text{-}N_2)_3$ (which was calculated to be the most stable structure); such a transformation is allowed by the symmetry constraints. However, only the anion of $Ni_3(\eta_t\text{-}N_2)_3$ assumes D_{3h} symmetry, whereas the structure $Ni_3(\eta^*_i\text{-}N_2)_3$ preserves its symmetry, C_{3h}.

After ionization, the BE per ligand molecule decreases by 19−34 kJ/mol. Whereas for the structures of Group I, this is a reduction of only 19−30%, for the structures of Group II the relative reduction is at least twice as large due to the small BE values of the neutral structures.

In general, variation of the charge of the complex changes pertinent characteristics in a systematic fashion. For all structures, the stability decreases on going from anionic to neutral to cationic systems; this trend correlates with the activation $\Delta(N{-}N)$ of the N−N bond (see above). Variation of the charge induces small changes in the bond lengths Ni−N, Ni−Ni, and N−N. As expected from the stability trend, the Ni−N distances are smallest in anionic, and largest in cationic structures: $R(Ni{-}N)^- < R(Ni{-}N) < R(Ni{-}N)^+$. The two stable structures with bridge bonding, $Ni_3(\mu_i\text{-}N_2)_3$ and $Ni_3(\mu_\perp\text{-}N_2)_3$, form exceptions. The changes $\Delta(Ni{-}Ni)$ do not exhibit a clear correlation with the charge of the systems.

We also optimized a structure imposing C_3 symmetry constraints. We started the geometric optimization with orientations of end-on bound ligands intermediate between those of the Group I structures $Ni_3(\eta^*_i\text{-}N_2)_3$ and $Ni_3(\eta_t\text{-}N_2)_3$ because that structure might change into either one of them. The optimization processes converged to the corresponding most stable structures for neutral, cationic, and anionic systems: $Ni_3(\eta^*_i\text{-}N_2)_3$, $Ni_3(\eta_t\text{-}N_2)_3$, and $Ni_3(\eta_i\text{-}N_2)_3$, respectively. As anionic systems, the structures $Ni_3(\eta_t\text{-}N_2)_3$ and $Ni_3(\eta_i\text{-}N_2)_3$ have essentially the same structural characteristic, with the exception of the angle θ, which is 180° for $Ni_3(\eta_i\text{-}N_2)_3$ (planar structure) but 171.3° for $Ni_3(\eta_t\text{-}N_2)_3$. The ligand BE values coincide with those obtained previously for the clusters of higher symmetry (Table 2). However, due to the different symmetry of the complex, the calculated vertical IP of neutral $Ni_3(\eta^*_i\text{-}N_2)_3$ in C_3 symmetry is 0.20 eV lower than that of the same complex with higher symmetry, C_{3h}. The orbital energies of the optimized neutral structures in C_3 and C_{3h} symmetry are identical, but they differ slightly for the corresponding cationic species.

C. Structure of $Ni_3(N_2)_4$ Complexes. We investigated five structures of the complex $Ni_3(N_2)_4$ (Figure 3a−c), two in C_{3v}

symmetry and one each in C_3, C_{2v}, and C_s symmetry. The only stable structure in C_{3v} symmetry is $Ni_3(\eta_t\text{-}N_2)_3(\mu_3\text{-}N_2)$ (Figure 3a), a singlet state with BE = 107 kJ/mol (Tables 2). In this structure a new type μ_3-N_2 of ligand appears, coordinated simultaneously to the three Ni atoms of the cluster. This ligand is relatively strongly bound to the cluster as indicated by the short value $R(Ni-N)^{br} = 184$ pm, the significant bond activation $\Delta(N-N)^{br} = 8.5$ pm, and the polarization as estimated by the difference, 0.19 e, between the Mulliken charges of the two N atoms of the μ_3-N_2 ligand (Table 2).

In fact, from the stability of $Ni_3(\eta_t\text{-}N_2)_3$, we determine the abstraction energy of the μ_3-N_2 ligand to 112 kJ/mol, somewhat larger than the average BE energy per ligand of the complex $Ni_3(\eta_t\text{-}N_2)_3$, 105 kJ/mol (Table 2). Thus, the $(\mu_3\text{-}N_2)$ ligand is more strongly bound in the complex $Ni_3(\eta_t\text{-}N_2)_3(\mu_3\text{-}N_2)$ than the $(\eta_t\text{-}N_2)$ ligands. On the other hand, from the R(Ni−N) distance of the η_t-N_2 ligands of $Ni_3(\eta_t\text{-}N_2)_3(\mu_3\text{-}N_2)$, which is 4 pm shorter than that in $Ni_3(\eta_t\text{-}N_2)_3$, one deduces a synergistic binding effect of $(\eta_t\text{-}N_2)$ and $(\mu_3\text{-}N_2)$ ligands in the larger complex.

Similarly to bridge-bonded μ_i-N_2 ligands in some of the $Ni_3(N_2)_3$ structures considered, the presence of a μ_3-N_2 ligand induces a significant elongation of the Ni−Ni bonds, Δ(Ni−Ni) = 22 pm; this value is much larger than that in the corresponding structure $Ni_3(\eta_t\text{-}N_2)_3$ without the μ_3-N_2 ligand where Δ(Ni−Ni) = 5 pm (Table 1). The charge of the metal cluster, $q(Ni_3) = 0.54$ e, is also significantly higher (Table 2).

Compared to other cationic systems, $Ni_3(\eta_t\text{-}N_2)_3(\mu_3\text{-}N_2)$ is very stable, $BE^+ = 87$ kJ/mol per ligand (Table 2). In fact, it is comparable to the most stable $Ni_3(N_2)_3$ complex $Ni_3(\eta_t\text{-}N_2)_3$ with $BE^+ = 86$ kJ/mol. However, as an anionic system, $Ni_3(\eta_t\text{-}N_2)_3(\mu_3\text{-}N_2)$ with $BE^- = 117$ kJ/mol is less stable than $Ni_3(\eta_t\text{-}N_2)_3$ with $BE^- = 146$ kJ/mol.

We optimized the structure of a Ni_3 cluster with four N_2 ligands also in C_3 symmetry with η-N_2 ligands off the vertical mirror planes of the Ni_3 cluster, but during the geometry optimization the structure returned to that of $Ni_3(\eta_t\text{-}N_2)_3(\mu_3\text{-}N_2)$ in C_{3v} symmetry described above. We also considered the structure $Ni_3(\mu_t\text{-}N_2)_3(\mu_3\text{-}N_2)$ in C_{3v} symmetry. However, during the optimization, the μ_3-N_2 ligand was abstracted from the cluster, and the μ_t-N_2 ligands moved toward the plane of the Ni_3 moiety forming a $Ni_3(\mu_i\text{-}N_2)_3$ complex.

The structure in C_{2v} symmetry, $Ni_3(\eta^*_i\text{-}N_2)_2(\eta_t\text{-}N_2)_2$ (Figure 3b), has two η_t-N_2 ligands attached to one of the Ni atoms, while the other two N_2 ligands η^*_i-N_2 are in the plane of the Ni_3 cluster, each coordinated to one of the remaining two Ni atoms. The average BE per N_2 molecule is 88 kJ/mol, 19 kJ/mol smaller than the value for the complex $Ni_3(\eta_t\text{-}N_2)_3(\mu_3\text{-}N_2)$. The Ni_3 moiety deviates slightly from equilateral geometry; the apex angle is 57.2°, and Ni−Ni bonds are extended by 1 and 11 pm. The values of R(Ni−N) and Δ(N−N) are similar to those of other η end-on bound N_2 ligands: R(Ni−N) = 181−188 pm and Δ(N−N) = 1.2−1.8 pm.

We considered a similar structure in C_s symmetry, $Ni_3(\eta^*_t\text{-}N_2)_2(\eta_t\text{-}N_2)_2$ (Figure 3c). In this structure the η^*_t-N_2 ligands are symmetry equivalent whereas the η_t-N_2 ligands are not. This structure can transform into either of the previous two structures of higher symmetry; however, during the optimization it goes to a local minimum with essentially the same BE, 90 kJ/mol, as the structure in C_{2v} symmetry. The geometry characteristics of both structures are very similar, except for the orientation of the η^*_t-N_2 ligands in the C_s structure, where these ligands are tilted by 169.3° with respect to the Ni_3 plane. The BE values per ligand of the structures with C_{2v} and C_s symmetry are 17−19 kJ/mol smaller than that of the complex with the μ_3-N_2 ligand, $Ni_3(\eta_t\text{-}N_2)_3(\mu_3\text{-}N_2)$.

D. Structure of $Ni_3(N_2)_5$ Complexes. We investigated five different structures with five N_2 ligands imposing C_{2v}, D_{3h}, and C_{3h} symmetry constraints (Figure 3d−g). The most stable of them is $Ni_3(\eta_i\text{-}N_2)_2(\mu_i\text{-}N_2)_3$ in C_{2v} symmetry (Figure 3d), a singlet state with BE = 102 kJ/mol (Table 2). The structure is planar with an apex angle Ni−Ni−Ni of 65.1°. One ligand is bound end-on to each of the two symmetry equivalent Ni atoms, at 182 pm as in the complex $Ni_3(\eta_i\text{-}N_2)_3$. The other three ligands are in μ_i positions; one of them is along the C_2 axis with $R(Ni-N)^{br} = 193$ pm, while the other two ligands feature different Ni−N distances $R(Ni-N)^{br}$, 183 and 196 pm, to the apex and the side Ni atoms, respectively (Table 1). Due to the presence of three bridging N_2 ligands, the positive charge of the Ni_3 moiety is significant, $q(Ni_3) = 0.62$ e, and these three ligands are strongly polarized, $q(N1) = -0.16$ e and $q(N2) = -0.05$ e, while both η_i-N_2 ligands are essentially neutral, $q(N1) = -0.01$ e and $q(N2) = 0.01$ e (Table 2).

The other structure in C_{2v} symmetry, $Ni_3(\eta_i\text{-}N_2)_3(\mu_i\text{-}N_2)_2$ (Figure 3e), has almost the same BE, 101 kJ/mol. The apex angle Ni−Ni−Ni is 61.2°. The two C_{2v} structures differ in the direction of the ligand, which coincides with the C_2 symmetry axis; in the previous case, it is coordinated to a Ni−Ni bond, in the present case to a Ni atom. Two symmetry equivalent η_i-N_2 ligands are oriented almost along the continuation of the "side" Ni−Ni bonds (Figure 3e). Similar to the other C_{2v} structure, the μ_i-N_2 ligands exhibit two different Ni−N distances, 183 and 189 pm. The positive charge of the Ni_3 moiety, 0.47 e, is somewhat smaller than that of $Ni_3(\eta_i\text{-}N_2)_2(\mu_i\text{-}N_2)_3$, because there are only two ligands in bridging positions (Table 2).

The next stable structure is $Ni_3(\eta^*_i\text{-}N_2)_3(\mu_3\text{-}N_2)_2$ in C_{3h} symmetry (Figure 3f), a singlet state with BE = 89 kJ/mol (Table 2). In this structure, there are two kinds of N_2 ligands: three bound to Ni atoms in linear end-on fashion, off the vertical mirror planes of the Ni_3 moiety, and two end-on bound ligands in 3-fold positions at both sides of the Ni_3 moiety. Here, at variance with the $Ni_3(\eta_t\text{-}N_2)_3(\mu_3\text{-}N_2)$ structure of $Ni_3(N_2)_4$, the two μ_3-N_2 ligands are bound weaker, and $R(Ni-N)^{br}$ is 19 pm longer than in $Ni_3(\eta_t\text{-}N_2)_3(\mu_3\text{-}N_2)$ (Table 1); concomitantly, the expansion of the Ni_3 moiety of $Ni_3(\eta^*_i\text{-}N_2)_3(\mu_3\text{-}N_2)_2$, Δ(Ni−Ni) = 11 pm, is only half as large as in $Ni_3(\eta_t\text{-}N_2)_3(\mu_3\text{-}N_2)$. The angle θ (Figure 2a) is 157.6°. The abstraction energy of the first μ_3-N_2 ligand calculated with respect to $Ni_3(\eta_t\text{-}N_2)_3(\mu_3\text{-}N_2)$ is only 17 kJ/mol, but the total abstraction energy of both μ_3-N_2 ligands is 95 kJ/mol with respect to $Ni_3(\eta^*_i\text{-}N_2)_3$, i.e., 47 kJ/mol per μ_3-N_2 ligand. In fact, the Ni−N distances for end-on bound N_2 ligands of the two structures $Ni_3(\eta^*_i\text{-}N_2)_3$ and $Ni_3(\eta^*_i\text{-}N_2)_3(\mu_3\text{-}N_2)_2$ are similar, 175 and 178 pm, respectively (Table 1). The activation of the μ_3-N_2 ligands, $\Delta(N-N)^{br} = 4.3$ pm, is also notably smaller than that in the $Ni_3(\eta_t\text{-}N_2)_3(\mu_3\text{-}N_2)$ structure, $\Delta(N-N)^{br} = 8.5$ pm (Table 1), but it is still significant compared to that of other structures with end-on bound N_2 ligands. Similarly to the structures containing bridge-bonded N_2 ligands, the Ni_3 moiety in the complex $Ni_3(\eta^*_i\text{-}N_2)_3(\mu_3\text{-}N_2)_2$ has a notable positive charge, $q(Ni_3) = 0.53$ e, and the polarization of the μ_3-N_2 ligands is large, $q(N1) = -0.17$ e and $q(N2) = -0.03$ e (Table 2).

Among the structures with five ligands, $Ni_3(\eta_i\text{-}N_2)_3(\mu_i\text{-}N_2)_2$ is most stable as a cationic system with $BE^+ = 86$ kJ/mol (Table 2). $Ni_3(\eta_i\text{-}N_2)_4(\mu_i\text{-}N_2)^-$ was identified as the most stable structure of the corresponding anionic system; that structure emerged from the geometry optimization of $Ni_3(\eta_i\text{-}N_2)_2(\mu_i\text{-}N_2)_3$ in C_{2v} symmetry, after the two μ_i ligands, coordinated to the symmetry-

equivalent Ni−Ni bonds, had moved to the apex Ni atom. The corresponding calculated BE^- per ligand is 111 kJ/mol, 9 kJ/mol higher than that in the neutral parent complex.

The other structure in D_{3h} symmetry, $Ni_3(\eta_i\text{-}N_2)_3(\mu_3\text{-}N_2)_2$ (Figure 3g), is similar to that of $Ni_3(\eta^*_i\text{-}N_2)_3(\mu_3\text{-}N_2)_2$; the BE per ligand is essentially the same (only 1 kJ/mol smaller, Table 2). The average abstraction energy of one μ_3-N_2 ligand of $Ni_3(\eta_i\text{-}N_2)_3(\mu_3\text{-}N_2)_2$ is 70 kJ/mol, 18 kJ/mol smaller than the average ligand BE. However, similarly to $Ni_3(\eta_t\text{-}N_2)_3(\mu_3\text{-}N_2)$, the η_i-N_2 ligands here are bound stronger [as judged by R(Ni−N) = 178 pm] than the η_i-N_2 ligands of the reference structure $Ni_3(\eta_i\text{-}N_2)_3$ without the two 3-fold bound ligands, where R(Ni−N) is 182 pm (Table 1).

The third structure modeled is $Ni_3(\mu_i\text{-}N_2)_3(\mu_3\text{-}N_2)_2$ (D_{3h} symmetry), where three N_2 ligands are in the plane of the Ni_3 moiety, coordinated to Ni−Ni bonds, and two ligands are 3-fold coordinated to the Ni_3 moiety as before. However, during the geometry optimization, the μ_3-N_2 ligands moved away from the Ni_3 cluster, resulting in the structure $Ni_3(\mu_i\text{-}N_2)_3$. From the decomposition of the structures $Ni_3(\mu_i\text{-}N_2)_3(\mu_3\text{-}N_2)_2$ and $Ni_3(\mu_t\text{-}N_2)_3(\mu_3\text{-}N_2)$, we hypothesize that structures with more than three bridge-bonded N_2 ligands (μ, μ^2, or μ_3) are unstable.

E. Structure of $Ni_3(N_2)_6$ Complexes. We investigated 15 structures of $Ni_3(N_2)_6$ in D_{3h} symmetry (Figure 4). One structure with C_{2v} symmetry and one with C_3 symmetry were also modeled, but in the course of the geometry optimization, they transform into structures with D_{3h} symmetry. Initial structures were derived from corresponding structures of the complex $Ni_3(N_2)_3$. The geometry and energetic characteristics of the optimized structures are shown in Tables 1 and 2. All these structures have closed-shell singlet states, except for $Ni_3(\eta_t\text{-}N_2)_6$ (Table 2), which is a triplet and features the third largest BE value. Obviously, six ligands suffice to quench the magnetism of Ni_3.[1,3]

One might have anticipated the structure $Ni_3(\eta^*_i\text{-}N_2)_6$ (Figure 4b) to be the most stable one for the complex $Ni_3(N_2)_6$, because it is analogous to the most stable structure $Ni_3(\eta^*_i\text{-}N_2)_3$ of the complex $Ni_3(N_2)_3$. However, the calculations yielded the structure $Ni_3(\eta_i\text{-}N_2)_3(\mu_i\text{-}N_2)_3$ (Figure 4a), with BE = 98 kJ/mol, as most stable; its two "parents" $Ni_3(\eta_i\text{-}N_2)_3$ and $Ni_3(\mu_i\text{-}N_2)_3$ are among the most stable structures of the complex $Ni_3(N_2)_3$. Weak steric interference between N_2 ligands is probably an important reason for this stability maximum; indeed, the values of R(Ni−N) are only slightly larger (2−5 pm) than those in the parent structures (Table 1). This weak mutual influence among the two types of ligands is consistent with their close values of average binding energies. The BE per ligand of $Ni_3(\eta_i\text{-}N_2)_3(\mu_i\text{-}N_2)_3$, 98 kJ/mol, is only 2−4 kJ/mol smaller than the BE values of the structures $Ni_3(\eta_i\text{-}N_2)_3$ and $Ni_3(\mu_i\text{-}N_2)_3$, 100 and 102 kJ/mol, respectively. Besides the weak interligand repulsion, a further reason for this near invariance of the ligand binding energies is connected with orbital interactions of the Ni_3 moiety and the N_2 ligands. Comparison of the Kohn−Sham valence level spectra of $Ni_3(\eta_i\text{-}N_2)_3(\mu_i\text{-}N_2)_3$ and $Ni_3(\eta_t\text{-}N_2)_6$ (see Section IV.A) suggests that the former complex is more stable due to both a stronger stabilization of the hybrid σ orbitals of N_2 ligands and a stronger π back-donation in the all-planar coordination of the "mixed" complex than in the tilted configuration.

The structure $Ni_3(\eta_i\text{-}N_2)_3(\mu_i\text{-}N_2)_3$ can be considered as a "parent" of the two most stable structures of the complex with five N_2 ligands, $Ni_3(\eta_i\text{-}N_2)_2(\mu_i\text{-}N_2)_3$ and $Ni_3(\eta_i\text{-}N_2)_3(\mu_i\text{-}N_2)_2$ (Figure 3d,e). Abstracting one ligand, we estimate the binding energies of one η_i-N_2 or μ_i-N_2 ligand of $Ni_3(\eta_i\text{-}N_2)_3(\mu_i\text{-}N_2)_3$ to be 79 and 85 kJ/mol, respectively.

In order of decreasing stability, the next structures of the complex $Ni_3(N_2)_6$ are $Ni_3(\eta^*_i\text{-}N_2)_6$ and $Ni_3(\eta_t\text{-}N_2)_6$ (Figure 4b,c). They are analogous to the two most stable structures with three ligands, $Ni_3(\eta^*_i\text{-}N_2)_3$ and $Ni_3(\eta_t\text{-}N_2)_3$, respectively, but with an average BE per N_2 ligand of 84 and 79 kJ/mol, respectively, the bonding is quite different: these BE values are 32 and 26 kJ/mol smaller than those of the analogous structures with three ligands, $Ni_3(\eta^*_i\text{-}N_2)_3$ and $Ni_3(\eta_t\text{-}N_2)_3$, respectively (Table 2). In both these structures of $Ni_3(N_2)_6$, each atom of the Ni_3 moiety is coordinated by two ligand molecules. This generates interligand steric repulsion, which leads to a change of the angle θ. For $Ni_3(\eta_t\text{-}N_2)_6$ that angle is 127.8°; thus, the deformation with respect to the reference structure with three ligands (θ = 162.4°) is significant. The Ni−N bonds are elongated by 5−9 pm with respect to the reference structures $Ni_3(\eta^*_i\text{-}N_2)_3$ and $Ni_3(\eta_t\text{-}N_2)_3$. As discussed above, besides the steric interaction, an orbital factor likely also contributes to the decrease of the N_2 binding energy in both structures with six ligand molecules.

The situation is similar for the corresponding cationic and anionic structures. The most stable structure as a cation is again $Ni_3(\eta_i\text{-}N_2)_3(\mu_i\text{-}N_2)_3$, with BE^+ = 78 kJ/mol. However, the difference in the values of BE^+ between the two most stable cationic structures is smaller than the BE difference of the corresponding neutral structures. $Ni_3(\mu_i\text{-}N_2)_3$, one of the "parent" structures of $Ni_3(\eta_i\text{-}N_2)_3(\mu_i\text{-}N_2)_3$, is least stable as a cation among all Group I structures of $Ni_3(N_2)_3$. The structures $Ni_3(\eta^*_i\text{-}N_2)_6$ and $Ni_3(\eta_t\text{-}N_2)_6$ have very similar BE^+ values, 66 and 65 kJ/mol, respectively. Two anionic structures have the same BE^- values: $Ni_3(\eta_i\text{-}N_2)_3(\mu_i\text{-}N_2)_3$ and $Ni_3(\eta_t\text{-}N_2)_6$ with BE^- = 108 kJ/mol (Table 2).

We also investigated one structure of $Ni_3(N_2)_6$ with C_3 symmetry, starting from initial orientations of the end-on bound ligands which are intermediate between the structures $Ni_3(\eta^*_i\text{-}N_2)_6$ and $Ni_3(\eta_t\text{-}N_2)_6$. However, during the geometry optimization, this structure transformed into that of $Ni_3(\eta_i\text{-}N_2)_3(\mu_i\text{-}N_2)_3$, corroborating the fact that the latter is the most stable neutral structure of $Ni_3(N_2)_6$. The structure $Ni_3(\eta_t\text{-}N_2)_6$ was also optimized in C_{2v} symmetry, starting from a geometry of the Ni_3 cluster that represents an isosceles triangle with an apex angle of 90°. During optimization, this structure changed into the corresponding structure $Ni_3(\eta_t\text{-}N_2)_6$ of D_{3h} symmetry. Because the $Ni_3(\eta_t\text{-}N_2)_3$ structure is more stable than that of $Ni_3(\eta_i\text{-}N_2)_3$, one might have expected that $Ni_3(\eta_t\text{-}N_2)_3(\mu_i\text{-}N_2)_3$ is more stable than $Ni_3(\eta_i\text{-}N_2)_3(\mu_i\text{-}N_2)_3$. However, during geometry optimization in C_{3v} symmetry, the structure $Ni_3(\eta_t\text{-}N_2)_3(\mu_i\text{-}N_2)_3$ transformed into $Ni_3(\eta_i\text{-}N_2)_3(\mu_i\text{-}N_2)_3$ (Figure 4a); this also holds for the corresponding cationic and anionic system.

The three structures just discussed, Figure 4a−c, have significantly larger binding energies than the other structures of the complex $Ni_3(N_2)_6$. Note that the ligand bonding in these structures comprises the types of bonding from Group I of the complexes $Ni_3(N_2)_3$.

Next in order of decreasing stability is the structure $Ni_3(\eta^2_i\text{-}N_2)_3(\mu_i\text{-}N_2)_3$ (Figure 4d), with an intermediate BE value of 64 kJ/mol (Table 2). This structure is a combination of two kinds of bonding: ligands side-on bonded to Ni atoms and ligands end-on bonded to Ni−Ni bonds. Here, the BE of the structure is essentially the same as that of the less stable structure $Ni_3(\eta^2_i\text{-}N_2)_3$, 63 kJ/mol, but smaller than the BE average of the two "parent" $Ni_3(N_2)_3$ structures. This BE value of $Ni_3(\eta^2_i\text{-}N_2)_3(\mu_i\text{-}N_2)_3$ is relatively large, concomitant with the fact that the distances $R(\text{Ni}-\text{N})^{br}$ of the bridge-bonded N_2 ligands (Table 1) are close to those of the most stable structure $Ni_3(\eta_i\text{-}N_2)_3(\mu_i\text{-}N_2)_3$. Steric constraints are reduced due to the elongation of

the Ni−N distance for the side-on bound ligands, and R(Ni−N) is 8 pm longer than in the structure $Ni_3(\eta^2_i\text{-}N_2)_3$. As a cation, the structure has a small BE^+ value, 46 kJ/mol; the bonding of the bridging ligands, $R(Ni-N)^{br+} = 226$ pm, is weak. The small BE^- value, 63 kJ/mol, of the anionic structure is similar to that of all other structures which comprise bridging ligands in the plane of the Ni_3 moiety.

The structure $Ni_3(\eta_i\text{-}N_2)_3(\mu^2{}_\perp\text{-}N_2)_3$ (Figure 4e) comprises N_2 ligands directed linearly to a Ni atom in the plane of the cluster and bridging ligands perpendicular to the plane of the cluster. Here, as found for the complex $Ni_3(\mu^2{}_\perp\text{-}N_2)_3$, expansion of the Ni_3 moiety in the presence of $\mu^2{}_\perp\text{-}N_2$ ligands leads to a destruction of the metal cluster; the optimized Ni−Ni distance is 138 pm larger than that in the bare Ni_3 cluster (Table 1). The average BE of N_2 ligands in this structure, 53 kJ/mol, is 11 kJ/mol larger than the BE of the complex $Ni_3(\mu^2{}_\perp\text{-}N_2)_3$, but considerably lower than the corresponding value of $Ni_3(\eta_i\text{-}N_2)_3$. A second minimum of this structure (not shown in the tables) with a less elongated Ni−Ni distance of 34 pm was also identified; however, the corresponding BE per ligand is 21 kJ/mol smaller.

The BE values of all other $Ni_3(N_2)_6$ structure are less than those of the corresponding "parent" structures of $Ni_3(N_2)_3$. There are four structures, where the bonding of the N_2 ligands cannot be considered as a combination of stable structures with three N_2 molecules, namely $Ni_3(\mu_t\text{-}N_2)_6$ (Figure 4f), $Ni_3(\eta^2{}_{||}\text{-}N_2)_6$ (Figure 4g), $Ni_3(\mu^2{}_{||}\text{-}N_2)_6$ (Figure 4h), and $Ni_3(\eta^{2*}{}_\perp\text{-}N_2)_6$ (Figure 4i). The most stable of them is $Ni_3(\mu_t\text{-}N_2)_6$, BE = 34 kJ/mol, where the ligands are bound end-on to Ni−Ni bonds. In the other three structures, both atoms of each ligand are bound to the Ni_3 cluster, but the corresponding BE values are smaller. $Ni_3(\eta^{2*}{}_\perp\text{-}N_2)_6$ is the least stable of these four structures because the steric constraint between N_2 ligands prevents them from coming close to the Ni_3 moiety. Only in this latter structure, the Ni_3 moiety carries a very small negative charge, $q(Ni_3) = -0.05$ e (Table 2).

There are several complexes where one type of ligand moved away from the metal cluster and the complex transformed into one of the $Ni_3(N_2)_3$ structures. Examples are $Ni_3(\eta^2{}_\perp\text{-}N_2)_3(\mu^2{}_\perp\text{-}N_2)_3$ (Figure 4j) and $Ni_3(\eta^2{}_i\text{-}N_2)_3(\mu^2{}_\perp\text{-}N_2)_3$ (Figure 4k). In both systems, the η^2 ligands are essentially not bound to the cluster and the complexes transform into the two local minima of $Ni_3(\mu^2{}_\perp\text{-}N_2)_3$ (Section III.B), as shown by the values of Δ(Ni−Ni), $\Delta(N-N)^{br}$, and q(N1) (Tables 1 and 2).

Other structures were unstable and could not be converged for various reasons. In the structures $Ni_3(\eta^2{}_i\text{-}N_2)_3(\mu^2{}_i\text{-}N_2)_3$ and $Ni_3(\eta_i\text{-}N_2)_3(\mu^2{}_i\text{-}N_2)_3$, the ligands are too close to each other; all N_2 ligands moved away from the Ni_3 moiety during structure optimization. No stable geometry was found for the moieties $Ni_3(\eta^2{}_\perp\text{-}N_2)_3(\mu_i\text{-}N_2)_3$ and $Ni_3(\eta^2{}_\perp\text{-}N_2)_3(\mu^2{}_i\text{-}N_2)_3$.

F. Structure of $Ni_3(N_2)_7$ Complexes. We modeled three structures of the complex with seven N_2 ligands: $Ni_3(\eta^*{}_t\text{-}N_2)_4(\eta^*{}_i\text{-}N_2)_2(\mu_3{}^*\text{-}N_2)$ (Figure 5a), $Ni_3(\eta^*{}_t\text{-}N_2)_6(\mu_3\text{-}N_2)$ (Figure 5b), and $Ni_3(\eta_i\text{-}N_2)_3(\mu_i\text{-}N_2)_3(\mu_3\text{-}N_2)$. The structures were derived from the second-most and the most stable structures with six ligands, $Ni_3(\eta^*{}_i\text{-}N_2)_6$ and $Ni_3(\eta_i\text{-}N_2)_3(\mu_i\text{-}N_2)_3$, respectively; the additional N_2 ligand is coordinated in μ_3 fashion to the Ni_3 cluster.

$Ni_3(\eta^*{}_t\text{-}N_2)_4(\eta^*{}_i\text{-}N_2)_2(\mu_3{}^*\text{-}N_2)$, in C_s symmetry, is the most stable structure among these three, with BE = 87 kJ/mol per ligand. Here, six of the ligands are bound end-on to a Ni atom; two ligands are located in the plane of the Ni_3 moiety, whereas the other four ligands are tilted with respect to the plane. These six ligands are somewhat closer to the corresponding Ni atoms, R(Ni−N) = 182−185 pm, compared to similar structures of $Ni_3(N_2)_6$, $Ni_3(\eta^*{}_i\text{-}N_2)_6$, and $Ni_3(\eta_t\text{-}N_2)_6$ with 184 and 187 pm (Table 1). The seventh ligand of $Ni_3(\eta^*{}_t\text{-}N_2)_4(\eta^*{}_i\text{-}N_2)_2(\mu_3{}^*\text{-}N_2)$ is in a 3-fold position; however, it is shifted to and tilted away from the base of the isosceles triangle Ni_3. The Ni−Ni distances of the Ni_3 moiety are extended by 21 and 29 pm with respect to the bare cluster; this expansion of the Ni_3 cluster is less than that in the other complex with seven ligands, $Ni_3(\eta^*{}_t\text{-}N_2)_6(\mu_3\text{-}N_2)$ (in C_{3v} symmetry), considered below, likely due to imposed symmetry constraints. During geometry optimization of the anionic form of $Ni_3(\eta^*{}_t\text{-}N_2)_4(\eta^*{}_i\text{-}N_2)_2(\mu_3{}^*\text{-}N_2)$, the $\mu_3{}^*\text{-}N_2$ ligand moves into the plane of the Ni_3 moiety and assumes a μ_i coordination, i.e., the anionic structure should be denoted as the $Ni_3(\eta^*{}_t\text{-}N_2)_4(\eta^*{}_i\text{-}N_2)_2(\mu_i\text{-}N_2)^-$ cluster.

During the geometry optimization of the structure $Ni_3(\eta_i\text{-}N_2)_3(\mu_i\text{-}N_2)_3(\mu_3\text{-}N_2)$, the $\mu_3\text{-}N_2$ ligand moves away from the cluster, to R(Ni−N) = 371 pm. Thus, $Ni_3(\eta_i\text{-}N_2)_3(\mu_i\text{-}N_2)_3(\mu_3\text{-}N_2)$ transforms into the complex $Ni_3(\eta_i\text{-}N_2)_3(\mu_i\text{-}N_2)_3$ and one separated N_2 molecule. Consequently, the calculated total BE of $Ni_3(\eta_i\text{-}N_2)_3(\mu_i\text{-}N_2)_3(\mu_3\text{-}N_2)$, 588 kJ/mol, is the same as the total BE of $Ni_3(\eta_i\text{-}N_2)_3(\mu_i\text{-}N_2)_3$.

The BE per ligand of the structure $Ni_3(\eta^*{}_t\text{-}N_2)_6(\mu_3\text{-}N_2)$ in C_{3v} symmetry is 78 kJ/mol (Table 2), i.e., the contribution of the ligand in the μ_3 position to the BE of the whole complex can be estimated to be 42 kJ/mol with respect to the isolated N_2 molecule and the $Ni_3(\eta^*{}_i\text{-}N_2)_6$ cluster; the latter is the stable structure closest to that of the $Ni_3(N_2)_6$ moiety that remains after abstraction of the $\mu_3\text{-}N_2$ ligand. However, the structure $Ni_3(\eta^*{}_t\text{-}N_2)_6(\mu_3\text{-}N_2)$ should not be interpreted as simple addition of a weakly bound seventh ligand; rather, there is a clear synergistic effect. With the $\mu_3\text{-}N_2$ ligand, the Ni−Ni distance of the complex extends substantially, Δ(Ni−Ni) = 53 pm; the BE per ligand is reduced compared to that of the complex $Ni_3(\eta^*{}_i\text{-}N_2)_6$, although the distance R(Ni−N) of the $\eta^*{}_i\text{-}N_2$ ligands is essentially the same, R(Ni−N) = 183 pm, as in the latter complex. The $\mu_3\text{-}N_2$ ligand carries a substantial negative charge and is strongly polarized, $q(N1) = -0.30$ e and $q(N2) = -0.06$ e. The cationic form of $Ni_3(\eta^*{}_t\text{-}N_2)_6(\mu_3\text{-}N_2)$ was calculated to be rather stable, with $BE^+ = 73$ kJ/mol, only 5 kJ/mol per ligand less than as a neutral structure. The corresponding structure without $\mu_3\text{-}N_2$ ligand, $Ni_3(\eta^*{}_i\text{-}N_2)_6$, features a much smaller BE^+ value, 55 kJ/mol (Table 2). The effect of the $\mu_3\text{-}N_2$ ligand on the BE per ligand is larger in the cationic form than in the neutral complex; this correlates with the reduced extension of the cationic Ni_3 moiety of $Ni_3(\eta^*{}_t\text{-}N_2)_6(\mu_3\text{-}N_2)$, Δ(Ni−Ni) = 24 pm, compared to the corresponding neutral system (Table 1).

G. Structure of $Ni_3(N_2)_8$ Complexes. We modeled three structures of the complex with eight ligands: $Ni_3(\eta^*{}_i\text{-}N_2)_6(\mu_3\text{-}N_2)_2$ (Figure 5c) and $Ni_3(\eta_i\text{-}N_2)_3(\mu_i\text{-}N_2)_3(\mu_3\text{-}N_2)_2$ in D_{3h} symmetry, as well as $Ni_3(\eta^*{}_i\text{-}N_2)_6(\eta_t\text{-}N_2)_2$ in C_{2v} symmetry. With N_2 ligands coordinated in μ_3 positions on each side of the Ni_3 moiety, these structures were constructed in an analogous fashion to those with seven N_2 molecules (see above).

For the complex $Ni_3(\eta^*{}_i\text{-}N_2)_6(\mu_3\text{-}N_2)_2$ (Figure 5c) in D_{3h} symmetry, the BE per ligand is 73 kJ/mol. The total BE of all N_2 ligands is 80 kJ/mol larger than the total BE of the six N_2 ligands in the structure $Ni_3(\eta^*{}_i\text{-}N_2)_6$; thus, the contribution of each ligand in μ_3 position can be estimated to 40 kJ/mol, practically the same as in $Ni_3(\eta^*{}_t\text{-}N_2)_6(\mu_3\text{-}N_2)$. Geometric parameters of linearly bound N_2 ligands of the structures $Ni_3(\eta^*{}_i\text{-}N_2)_6(\mu_3\text{-}N_2)_2$ (Figure 5c) and $Ni_3(\eta^*{}_t\text{-}N_2)_6(\mu_3\text{-}N_2)$ (Figure 5b) are similar (Table 1); only the two $\mu_3\text{-}N_2$ ligands of $Ni_3(\eta^*{}_i\text{-}N_2)_6(\mu_3\text{-}N_2)_2$ are coordinated somewhat farther away, $R(Ni-N)^{br} = 209$ pm, than in the seven-coordinated complex, $R(Ni-N)^{br} = 194$ pm (Table 1). The expansion of the Ni_3

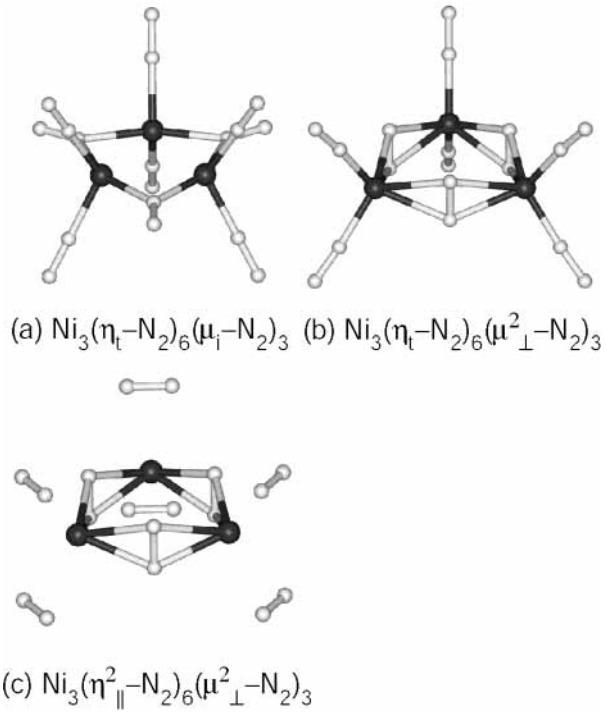

Figure 6. Structures of the Ni_3 moiety with nine N_2 ligands: (a) $Ni_3(\eta_t\text{-}N_2)_6(\mu_i\text{-}N_2)_3$, (b) $Ni_3(\eta_t\text{-}N_2)_6(\mu^2{}_\perp\text{-}N_2)_3$, and (c) $Ni_3(\eta^2{}_{||}\text{-}N_2)_6(\mu^2{}_\perp\text{-}N_2)_3$.

moiety of $Ni_3(\eta^*{}_i\text{-}N_2)_6(\mu_3\text{-}N_2)_2$, $\Delta(Ni-Ni) = 43$ pm, is less than that in the complex with seven N_2 ligands.

The structure $Ni_3(\eta^*{}_i\text{-}N_2)_6(\mu_3\text{-}N_2)_2$ is very stable as a cationic system, $BE^+ = 69$ kJ/mol, but this BE^+ value is smaller than that of the cation of $Ni_3(\eta^*{}_i\text{-}N_2)_6(\mu_3\text{-}N_2)$.

In the other structure with eight ligands, $Ni_3(\eta_i\text{-}N_2)_3(\mu_i\text{-}N_2)_3(\mu_3\text{-}N_2)_2$, the two $\mu_3\text{-}N_2$ ligands moved away from the cluster, and a complex with six ligands remained, similarly to the analogous structure with seven ligands, $Ni_3(\eta_i\text{-}N_2)_3(\mu_i\text{-}N_2)_3(\mu_3\text{-}N_2)$. We also modeled one $Ni_3(N_2)_8$ structure in lower (C_{2v}) symmetry, $Ni_3(\eta^*{}_i\text{-}N_2)_6(\eta_t\text{-}N_2)_2$, where the $\eta_t\text{-}N_2$ ligands are coordinated to one of the Ni centers. However, during the optimization, the Ni_3 moiety decomposed into two $Ni(N_2)_2$ and one $Ni(N_2)_4$ species, although that structure lies only 16 kJ/mol lower than $Ni_3(\eta^*{}_i\text{-}N_2)_6(\mu_3\text{-}N_2)_2$.

H. Structure of $Ni_3(N_2)_9$ Complexes. We investigated five structures of the Ni_3 moiety with nine ligand molecules, imposing D_{3h} symmetry (Figure 6). The most stable of them is $Ni_3(\eta_t\text{-}N_2)_6(\mu_i\text{-}N_2)_3$ (Figure 6a), BE = 72 kJ/mol (Table 2). This structure combines two end-on bound ligands at each Ni center and one end-on bound ligand at each Ni−Ni bond. The bonding of $\eta_t\text{-}N_2$ ligands is slightly weaker than that of the ligands in the complex $Ni_3(\eta_t\text{-}N_2)_6$ without bridge-bonded ligands (Figure 4c); R(Ni−N) is 2 pm longer and the N−N bonds are 0.1 pm less activated than in the reference structure $Ni_3(\eta_t\text{-}N_2)_6$. On the other hand, the coordination of the two $\mu_i\text{-}N_2$ ligands is much weaker than that in $Ni_3(\mu_i\text{-}N_2)_3$ (Figure 2d); the distance $R(Ni-N)^{br}$ is 9 pm longer than that in the latter structure and the activation Δ(N−N) is 1.7 pm smaller. The value of Δ(Ni−Ni), 41 pm, is quite large; thus, the structure should be considered as a complex of three Ni atoms each ligated by two N_2 molecules. The whole structure is held together by the three bridge-bonded μ_i-type ligands.

In the cationic complex, the metal moiety expands significantly less, $\Delta(Ni-Ni)^+ = 28$ pm, and its BE^+ is relatively high, 63 kJ/mol. Here, the $\mu_i\text{-}N_2$ ligands are located at the same distance as in the neutral complex, $R(Ni-N)^+ = 196$ pm, but the $\eta_t\text{-}N_2$ ligands are 8 pm farther away than in the neutral structure. The BE per ligand molecule of the anionic structure, $BE^- = 75$ kJ/mol, is only 3 kJ/mol larger than the corresponding value of the neutral structure. This small increase of the BE per ligand in the anionic structures is typical for all complexes which contain bridge-bonded $\mu_i\text{-}N_2$ ligands in the plane of the cluster, e.g. $Ni_3(\mu_i\text{-}N_2)_3$, $Ni_3(\eta_i\text{-}N_2)_3(\mu_i\text{-}N_2)_3$, and $Ni_3(\eta^2{}_i\text{-}N_2)_3(\mu_i\text{-}N_2)_3$ (Figures 2d, 4a, and 4d). As an anionic complex, the Ni_3 moiety of $Ni_3(\eta_t\text{-}N_2)_6(\mu_i\text{-}N_2)_3$ expands more, $\Delta(Ni-Ni)^- = 51$ pm, than in the neutral structure (Table 1).

The next structure to be discussed is $Ni_3(\eta_t\text{-}N_2)_6(\mu^2{}_\perp\text{-}N_2)_3$ (Figure 6b) with BE = 58 kJ/mol. It differs from the previous structure by reorienting the bridge-bonded N_2 ligands perpendicular to the Ni_3 plane. The value of R(Ni−N), 185 pm, for the $\eta_t\text{-}N_2$ ligands is slightly smaller than the corresponding value of the structure $Ni_3(\eta_t\text{-}N_2)_6$, 187 pm (Table 1); the corresponding values of the cationic and anionic structures of $Ni_3(\eta_t\text{-}N_2)_6(\mu^2{}_\perp\text{-}N_2)_3$ are also similar. Interestingly, both in the neutral and in the charged structures the Ni−Ni distance expands by more than 150 pm; in other words, the Ni−Ni bonds are broken forming three $Ni(N_2)_2$ species and the stability of the whole structure is due to the bonds mediated by bridging ligands $\mu^2{}_\perp\text{-}N_2$.[35] We also separately investigated the complexes $Ni(N_2)_2$ which turned out to be stable with BE = 164 kJ/mol per N_2. Such species were observed experimentally with IR and Raman spectroscopy.[36]

The third stable structure is $Ni_3(\eta^2{}_{||}\text{-}N_2)_6(\mu^2{}_\perp\text{-}N_2)_3$ (Figure 6c), but it features a much smaller BE value, 24 kJ/mol, than the first two structures considered. The structure differs from the previous ones by the orientation of the η-ligands, which here are oriented parallel to the plane of the Ni_3 triangle, symmetrically above and below each Ni atom. Both types of bonding, $\eta^2{}_{||}\text{-}N_2$ and $\mu^2{}_\perp\text{-}N_2$, are not very strong; thus, the BE values of neutral, cationic, and anionic structures are all small. Although both types of ligands, $\eta^2{}_{||}\text{-}N_2$ and $\mu^2{}_\perp\text{-}N_2$, are bound weaker to the metal centers compared to the two parent structures $Ni_3(\eta^2{}_{||}\text{-}N_2)_6$ and $Ni_3(\mu^2{}_\perp\text{-}N_2)_3$, respectively, the Ni_3 moiety is considerably expanded, and the optimized distances between Ni atoms are elongated by more than 130 pm for the neutral and the ionic structures compared (to bare Ni_3 cluster); thus, Ni−Ni bonds again are broken.

In the structures with nine ligands, bridge-bonded ligands carry significantly larger negative charges, −0.14 to −0.22 e, than N_2 ligands bound to a Ni atom, which are essentially neutral, with charges from 0.01 to −0.01 e.

In the forth structure modeled, $Ni_3(\eta_t\text{-}N_2)_6(\eta_i\text{-}N_2)_3$, the $\eta^2{}_i\text{-}N_2$ ligands moved away from the cluster during geometry optimization. Hence, this structure transforms to a $Ni_3(N_2)_6$ complex. Pertinent structural characteristics, R(Ni−N), Δ(Ni−Ni), and Δ(N−N), of the $\eta_t\text{-}N_2$ ligands exhibit the same values as in $Ni_3(\eta_t\text{-}N_2)_6$. The total BE of this structure $Ni_3(\eta_t\text{-}N_2)_6(\mu_i\text{-}N_2)_3$ is 477 kJ/mol, i.e., practically the same as for the complex $Ni_3(\eta_t\text{-}N_2)_6$, 476 kJ/mol. Another structure studied, $Ni_3(\eta_t\text{-}N_2)_6(\eta^2{}_i\text{-}N_2)_3$, combines ligands end-on coordinated tilted to the Ni atom and ligands bound side-on to Ni atom; however, during the geometry optimization, all N_2 ligands dissociated from the Ni_3 moiety. These findings for the latter two structures $Ni_3(\eta_t\text{-}N_2)_6(\eta_i\text{-}N_2)_3$ and $Ni_3(\eta_t\text{-}N_2)_6(\eta^2{}_i\text{-}N_2)_3$ suggest that an atom of Ni_3 is not able to coordinate more than two ligands in η-fashion.

I. Structure of $Ni_3(N_2)_{12}$. We investigated one structure with twelve N_2 ligands, $Ni_3(\eta_t\text{-}N_2)_6(\eta^*{}_i\text{-}N_2)_6$. It combines structural elements of $Ni_3(\eta_t\text{-}N_2)_6$ and $Ni_3(\eta^*{}_i\text{-}N_2)_6$; these are second and third in the order of decreasing stability among the complexes

with six N_2 ligands. However, during the geometry optimization, the structure dissociated into three mononuclear complexes $Ni(N_2)_4$ of tetrahedral symmetry. Therefore, we also studied the complex $Ni(N_2)_4$ separately in C_{2v} symmetry. Geometry optimization restores T_d symmetry; all distances are the same as in the species obtained from the decomposition of the model structure $Ni_3(\eta_t\text{-}N_2)_6(\eta^*_i\text{-}N_2)_6$, in particular $R(Ni-N) = 187$ pm. The calculated BE per N_2 ligand of the complex $Ni(N_2)_4$ is 110 kJ/mol.

IV. Discussion

A. Bonding of the N_2 Ligands to the Ni_3 Cluster. To shed light on the formation of the complex between the cluster Ni_3 and N_2 ligands, we considered how the energy of the valence orbitals (3d and 4s of Ni atoms; 2s and 2p of N atoms) varied in selected complexes relative to the bare Ni_3 cluster and free N_2 molecules. We considered the most stable complex with six N_2 ligands, $Ni_3(\eta_i\text{-}N_2)_3(\mu_i\text{-}N_2)_3$, as well as its "parent" complexes with three ligands, $Ni_3(\eta_i\text{-}N_2)_3$ and $Ni_3(\mu_i\text{-}N_2)_3$. For comparison, we also discuss two complexes, $Ni_3(\eta_t\text{-}N_2)_3$ and $Ni_3(\eta_t\text{-}N_2)_6$, with a tilted orientation of linearly bound ligands.

N_2 ligands bind to a Ni_3 cluster in a similar way as CO in transition complexes.[3,6a,b,d,e] In response to the metal cluster, the 4σ and 5σ orbitals of N_2 are polarized and rehybridized. Interaction with the valence orbitals of the Ni atoms stabilizes the polarized N_2 σ orbitals, especially the one directed toward the metal cluster which we refer to as the N_2 4σ-derived orbital.[37] On the other hand, π-back-donation from occupied Ni d-orbitals to the antibonding π^* orbital of the N_2 ligands stabilizes the participating d-orbitals of Ni. Orbital mixing in general is small, i.e., metal contributions to ligand-derived MOs and N_2 contributions to metal orbitals are 10−12% at most. Such a clear separation of orbitals is already known from the bonding of CO to neutral nickel clusters.[3,6a,b,d,e] In the clusters considered here, the highest lying valence orbital of the ligands is more than 3 eV more stable than the valence orbitals of the Ni_3 cluster. Thus, σ bonding and π back-bonding can be monitored by the stabilization of the N_2 σ orbitals and d-orbitals, respectively.

We first consider the energy variation of the ligand orbitals. In open-shell structures, energies of corresponding ligand orbitals with opposite spin split at most 0.03 eV; only the 5σ-like and some of the 4σ-like orbitals of the cluster $Ni_3(\eta_t\text{-}N_2)_6$ show energy differences of up to 0.1 eV. The orbital structure of the complexes with three linearly bound ligands, $\eta_i\text{-}N_2$ and $\eta_t\text{-}N_2$, is the same: (i) the lower lying 4σ-derived orbitals (with dominant contributions of the lone pair of the N atom coordinated to a metal atom) feature a pronounced stabilization by 2.0 eV with respect to the 4σ MO of free N_2; (ii) the higher lying 5σ-derived orbitals, mainly of lone-pair character at the N atom distant from the Ni_3 moiety, are slightly stabilized, by 0.4 eV with respect to 5σ MO of N_2; and (iii) the 1π orbitals of N_2 are stabilized by only 0.3 eV. In bridge-bound ligands, $\mu_i\text{-}N_2$, the 4σ-like orbitals (with participation of the N atoms oriented to Ni−Ni bonds) are stabilized even more than in the linear ligands, by 2.2−2.9 eV, while the stabilization the 5σ-like and π orbitals is much weaker or even vanishing, 0.4 and 0.0 eV, respectively.

The orbital spectrum of the complex $Ni_3(\eta_i\text{-}N_2)_3(\mu_i\text{-}N_2)_3$ essentially looks like a superposition of the spectra of the two parent structures with three ligands; the 4σ and 5σ orbitals of the $\mu_i\text{-}N_2$ ligands are slightly more stabilized. The orbital spectrum of the complex with six equivalent ligands, $Ni_3(\eta_t\text{-}N_2)_6$, also remains similar to the corresponding complex with three ligands, $Ni_3(\eta_t\text{-}N_2)_3$; however, the 4σ-like orbitals of the three additional ligands are destabilized by 0.5 eV with respect to the complex $Ni_3(\eta_t\text{-}N_2)_3$. This is likely one of the reasons why the $Ni_3(N_2)_6$ complex with two types of ligands exhibits a higher stability than a complex with only one type of ligand (see Section III.E).

The analysis of the changes in the orbitals of the Ni atoms is more complicated as Ni d and s orbitals are to some extent hybridized. In general, after coordination of the ligands, Ni_3 MOs with strong 4s participation are notably destabilized (above the d manifold), similar to the findings in nickel carbonyl complexes and clusters.[3,6a,b,d,e] In the complexes with only η-coordinated ligands, the Ni 4s-derived levels shift about 0.5 eV upward, whereas in the complexes $Ni_3(\mu_i\text{-}N_2)_3$ and $Ni_3(\eta_i\text{-}N_2)_3(\mu_i\text{-}N_2)_3$ the 4s-like orbitals are empty. Thus, the σ-bonding of η-coordinated N_2 ligands is not strong enough to push the 4s orbital beyond the Fermi level as in the case of CO. Due to π-back-donation, most of the Ni 3d orbitals in the complexes are stabilized after coordination; back-donation is stronger for planar structures with optimal orbital overlap.

The N−N bonds of μ_i-bound ligands are more activated with respect to free N_2, $\Delta(N-N) = 4.8$ pm, than in η-coordinated ligands and the Ni_3 moiety carries a large positive charge, e.g. $q(Ni_3) = 0.72$ e in the complex $Ni_3(\mu_i\text{-}N_2)_3$ (Tables 1 and 2). The transfer of electronic density from the Ni_3 moiety to the coordinated N atoms results in a large polarization of the ligands. The findings for other structures with $\mu\text{-}N_2$ ligands are similar.

In the structure $Ni_3(\mu^2{}_\perp\text{-}N_2)_3$, π-orbitals of N_2 perpendicular to the N−N bond participate in Ni−N bonding; as a result, the order of the N−N bond decreases and the N_2 ligands are significantly activated, $\Delta(N-N) = 9.5$ pm; also, the charge of the Ni_3 cluster is substantial: $q(Ni_3) = 1.21$ e.

As an analysis of the charge distribution shows, the positive charge of the Ni_3 moiety is smaller for linearly bound $\eta\text{-}N_2$ ligands, 0.12−0.18 e, due to a slight domination of the π-back-donation over the σ-donation, whereas in the complexes with other types of $\eta\text{-}N_2$ ligands the charge of Ni_3 cluster increases up to 0.39 e (Table 2). For stable complexes including $\mu\text{-}N_2$ ligands as well as for mixed complexes the charge of the Ni_3 moiety is between 0.40 and 1.21 e (Table 2), which reflects differences in the bonding mechanism of the bridging ligands, e.g. with some ionic contributions to the Ni−N bonds. Interestingly, the strongest charge separation appears always for $\mu^2{}_\perp\text{-}N_2$ coordination where $q(Ni_3) = 0.75-1.21$ e. The most prominent exception from these considerations is the complex $Ni_3(\eta^{2*}{}_\perp\text{-}N_2)_6$, where the charge of the Ni_3 moiety is negative, −0.15 e, i.e., each N_2 ligand carries a tiny positive charge of 0.02 e. This opposite direction of charge separation could originate from the distant location of the ligands [they are 32 pm farther from the Ni atoms compared to the corresponding complex with three ligands, $Ni_3(\eta^2{}_\perp\text{-}N_2)_3$] and the lack of suitably oriented occupied 3d orbitals of the Ni atoms.

Half of the considered structures with three N_2 ligands, $Ni_3(\eta_t\text{-}N_2)_3$, $Ni_3(\eta_i\text{-}N_2)_3$, $Ni_3(\eta^2{}_i\text{-}N_2)_3$, and $Ni_3(\mu^2{}_i\text{-}N_2)_3$, feature a triplet state, similarly to the bare Ni_3 cluster. However, only one structure of the six-coordinated complex $Ni_3(N_2)_6$ is a triplet: $Ni_3(\eta_t\text{-}N_2)_6$; all other structures are singlets (Table 2). Only one structure of $Ni_3(N_2)_9$ has a triplet state, $Ni_3(\eta_t\text{-}N_2)_6(\eta_i\text{-}N_2)_3$; this is not unexpected as, during geometry optimization, this structure transforms into $Ni_3(\eta_t\text{-}N_2)_6$, which is also paramagnetic. Reduction of the multiplicity with increasing numbers of ligands can be rationalized by the filling of the Ni 3d manifold because Ni 4s and 4p levels are pushed up in energy and their occupation is reduced.[1,3,6] To corroborate this argument, we consider how the Ni 3d populations of ligated clusters changes

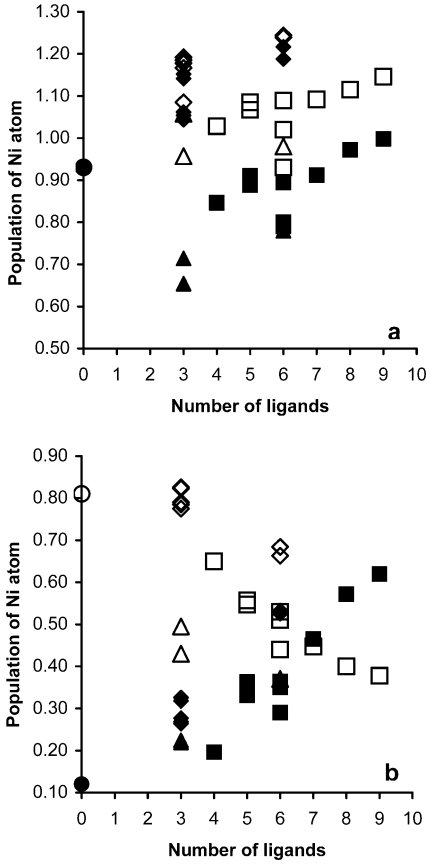

Figure 7. Effective 3d, 4s, and 4p populations of a Ni center in complexes with different numbers of ligands and coordination mode: η (rhombus), μ (triangles), and mixed (squares). (a) Population deficit of the 3d shell with respect to the nominal value 10 (empty symbols) and sum of 4s and 4p populations (filled symbols); (b) 4s (open symbols) and 4p (filled symbols) populations.

with the number of ligands and their type of coordination (Figure 7a). The 3d population of the bare Ni_3 cluster is 9.07 e, i.e., 0.93 e of the 3d orbitals remains unfilled at the expense of the 4s and 4p occupations, 0.81 and 0.12 e, respectively. The Ni 3d population of ligated clusters is reduced from the maximum value, 10 e, not only by population of Ni 4s and 4p levels, but also by overall transfer of electron density to the ligands. Figure 7a shows the unfilled part of the Ni 3d manifold (empty symbols) and the sum of Ni 4s and 4p populations (filled symbols). In all cases, the "electron hole" population of the 3d levels is equal or larger than that in the bare Ni_3 cluster. For complexes with η-type ligands (empty rhombus), the remaining electrons occupy Ni at the 4s and 4p manifolds (filled rhombus), as can be seen from the close location of the two types of symbols in Figure 7a. The 3d manifold is to a notable amount unfilled, 1.09−1.24 e, and most of these structures are triplets as expected. In most of the other complexes, with μ ligands (triangles) and mixed complexes with less than 8 ligands (squares), the sum of 4s and 4p populations is smaller than that in the bare Ni_3 cluster and also less than that of the unfilled part of the 3d manifold, accompanied by a large positive population of the Ni_3 moiety. All these complexes are singlets, although in some of them the unfilled part of the 3d manifold is equal or larger than 1 e. The quenching of the magnetic state in these structures could originate from the transfer of electron density from the Ni 3d levels to the ligands, accompanied by a rehybridization of the Ni 3d, 4s, and 4p orbitals to overlap more efficiently with ligand orbitals, especially of μ-type.

It is also interesting to follow how populations of Ni 4s (open symbols) and 4p (filled symbols) levels vary depending on the number of ligands and their type of coordination (Figure 7b). Complexes with η-type ligands (empty rhombus) feature the highest occupation of 4s orbitals, 0.66−0.83 e (similar to the bare cluster shown as a circle), whereas in complexes with μ-type ligands (empty triangles) the 4s population is are much smaller, 0.37−0.50 e. In complexes with more than three ligands, but of either coordination type, η and μ (empty squares), the Ni 4s population decreases with the number of ligands, from 0.65 e in $Ni_3(\eta_t\text{-}N_2)_3(\mu_3\text{-}N_2)$ to 0.38 e in $Ni_3(\eta_t\text{-}N_2)_6(\mu_i\text{-}N_2)_3$. In a similar fashion, the 4p population of complexes with only η ligands (filled rhombus) is larger than that in other structures with the same number of ligands. However, at variance with the general trend of the 4s orbitals, the 4p occupation (filled squares) increases substantially with the number of ligands, up to 0.62 e in $Ni_3(\eta_t\text{-}N_2)_6(\mu_i\text{-}N_2)_3$. This increase of the 4p population with the number of ligands may reflect the need for more hybridization at the Ni centers to achieve an overlap with an increasing number of (σ-donating) ligands.

As mentioned in Section II, we checked selected structures by lowering the symmetry constraint and discussed these results in Section III. In particular, we inspected all neutral structures for the presence of a degenerate partially occupied HOMO, to identify candidates for a first-order Jahn−Teller distortion; we found two such cases: $Ni_3(\eta_i\text{-}N_2)_3$ in D_{3h} and $Ni_3(\eta_t\text{-}N_2)_3$ in C_{3v}. Both structures are triplets with configurations $(a_1'')^1(e')^3$ (D_{3h}) or $a_2^1e^3$ (C_{3v}) where the HOMO is a singly occupied spin−orbital of e-type. The degeneracy of the e-type HOMO orbital of $Ni_3(\eta_i\text{-}N_2)_3$ or $Ni_3(\eta_t\text{-}N_2)_3$ structures can be removed by reduction of symmetry to C_{2v} or lower, i.e., by removing the 3-fold axis. Forced distortion of the isolateral triangle in $Ni_3(\eta_i\text{-}N_2)_3$ in different directions indeed results in a splitting of the two spin−orbitals originating from the e-type HOMO in D_{3h} symmetry, one of which is occupied. However, either the obtained structure is less stable than the isolateral triangle, or the SCF procedure did not converge even when fixed to the electronic configuration, which corresponds to that of the D_{3h} structure. The other neutral structures do not have degenerate partially unfilled HOMO levels, so they are not candidates for a first-order Jahn−Teller distortion. Due to the open-shell character of the charged structures, there are more ionic complexes with partially unfilled HOMO levels that may undergo this type of distortion.

The possibility of a second-order Jahn−Teller effect was first checked by partial distortion of the symmetric structures of the most stable structures in D_{3h} or C_{3h} symmetry with three, four, and six ligands. As reported in the corresponding parts of Section III, in all cases reoptimization in C_3 symmetry restored the corresponding structures of higher symmetry. We also considered a further symmetry reduction by removing the 3-fold axis in selected structures of the complex with four to seven ligands, with subsequent reoptimization in C_{2v} or C_s symmetry. For the complex $Ni_3(N_2)_4$, reduction of symmetry resulted in two new structures (Figure 3b,c), but both were less stable than the corresponding structures of higher (C_{3v}) symmetry (Figure 3a). The complex $Ni_3(\eta_t\text{-}N_2)_6$ was also modeled in C_{2v} symmetry, but optimization restored the structure of higher symmetry (D_{3h}). For the complexes $Ni_3(N_2)_5$ and $Ni_3(N_2)_7$, a change of symmetry constraints to C_{2v} and C_s, respectively, resulted in more stable new structures, by 9−13 kJ/mol per ligand. These new structures (Figures 3d and 5a) were used in the following as the most stable structures when deriving the overall product distribution; see Section IV.D.

B. Binding Energies. For the most stable structures of the complexes studied, the value of the BE per ligand molecule

decreases from 116 kJ/mol for $Ni_3(N_2)_3$ to 72 kJ/mol for $Ni_3(N_2)_9$ as the number of N_2 ligands increases. As no experimental binding energy of N_2 on a Ni_3 cluster has been reported so far, we compare our calculated values per ligand with the experimental adsorption energy of N_2 molecules on Ni surfaces,[38] 25−59 kJ/mol, or on clusters Ni_n (n = 19−71), 67−84 kJ/mol;[14d] this comparison corroborates the expectation that the BE per ligand increases when the bond saturation of the metal atoms decreases with the size of the metal moiety. The BE of the structures with three ligands is mainly determined by the type of ligand bonding; η-type (end-on) binding to Ni atoms is strongest. Among the three types of such bonding η_i, η^*_i and η_t, η^*_i are most stable, i.e., when the ligand molecules are oriented linearly toward a Ni atom, but are located off the σ_v reflection plane of the Ni_3 moiety (Figures 2a and 4b). End-on bonding to a Ni−Ni bond, μ-type, is also stable (Figures 2c and 4a,d), followed in stability by side-on bonding to a Ni atom, η^2, and then by μ^2, side-on coordination to a Ni−Ni bond as the least stable type of bonding: BE(η) > BE(μ) > BE(η^2) > BE(μ^2).

The BE of the N_2 ligands coordinated end-on in the μ_3 position depends on the number of other ligands and their orientation. The contribution of μ_3-N_2 ligands to the total BE of the complex can be estimated by the difference between corresponding complexes with and without μ_3 ligands. The values obtained in this way for the neutral structures vary between 113 and 40 kJ/mol per coordinated molecule, i.e., the strength of these of bonds is similar to that of η and μ types.

In addition to the orientation of the ligands, steric repulsion between N_2 ligands also influences the BE for structures with six ligand molecules. The structures of the complexes with more than six ligands are mainly determined by the minimum distances between N_2 ligands, due to the large number of adsorbed N_2 units around the small Ni_3 moiety. In these structures, some of the N_2 ligands are often at large distances from the metal particle: $Ni_3(\eta_t\text{-}N_2)_6(\eta_i\text{-}N_2)_3$, $Ni_3(\eta_t\text{-}N_2)_6(\eta^2{}_i\text{-}N_2)_3$, $Ni_3(\eta_i\text{-}N_2)_3(\mu_i\text{-}N_2)_3(\mu_3\text{-}N_2)$, and $Ni_3(\eta_i\text{-}N_2)_3(\mu_i\text{-}N_2)_3(\mu_3\text{-}N_2)_2$. Also, to provide more space around the Ni_3 unit, the distance between Ni atoms increases by more than 40 pm, as in $Ni_3(\eta^*_i\text{-}N_2)_6(\mu_3\text{-}N_2)$, $Ni_3(\eta^*_i\text{-}N_2)_6(\mu_3\text{-}N_2)_2$, $Ni_3(\eta^2{}_{||}\text{-}N_2)_6(\mu^2{}_\perp\text{-}N_2)_3$, $Ni_3(\eta_t\text{-}N_2)_6(\mu^2{}_\perp\text{-}N_2)_3$, and $Ni_3(\eta_t\text{-}N_2)_6(\mu_i\text{-}N_2)_3$. In the structure $Ni_3(\eta_t\text{-}N_2)_6(\eta^*_i\text{-}N_2)_6$, the complex dissociates completely. With a few exceptions, all structures are most stable as anions and least stable as cations: $BE^- > BE > BE^+$. The exceptions are $Ni_3(\mu_i\text{-}N_2)_3$, $Ni_3(\eta^2{}_{||}\text{-}N_2)_3(\mu_i\text{-}N_2)_3$, and $Ni_3(\eta^2{}_{||}\text{-}N_2)_6(\mu^2{}_\perp\text{-}N_2)_3$, where the BE values per atom for the anionic structures are essentially the same as in the corresponding neutral structures (in fact, 1−3 kJ/mol smaller).

η_i-type ligands contribute to the stabilization due to their particularly suitable locations. η^*_i bonding allows mixing only with ligands in μ_3 position (Figures 2a and 4b). The orientation of the N_2 molecules with η_t bonding, out of the plane of the Ni_3 moiety, admits bridge bonding of other ligands; this type of bonding is especially stable in cationic and anionic structures.

The most stable bridge-bound ligands, μ_i, occur in the most stable structures of the complexes $Ni_3(N_2)_5$, $Ni_3(N_2)_6$, and $Ni_3(N_2)_9$; but as cations and especially as anions, they are less stable than other structures of Group I structures of $Ni_3(N_2)_3$.

Depending on the other ligands in the complex, μ_3 is a stable type of bonding in combination with linearly bound ligands in the plane of the cluster, η_i-N_2 or η^*_i-N_2 (as in the stable complexes with five, seven, and eight ligands), and tilted η_t-N_2 ligands (as in the complex with four ligands). However, complexes with μ_3-N_2 ligands are unstable when other ligands are coordinated in bridging positions in the plane of the Ni_3 moiety. All structures containing μ_3-N_2 ligands typically feature a large expansion of the Ni_3 moiety, Δ(Ni−Ni) = 10−53 pm for neutral structures, and a large activation and polarization of the N−N bond of the μ_3-N_2 ligand, Δ(N−N) = 3.9−6.3 pm.

$\eta^2{}_\perp$-type bonding is stable only in the complex $Ni_3(\eta^2{}_\perp\text{-}N_2)_3$, but we did not find any complex where such ligands were combined with bridge-bound ligands. In such structures, the $\eta^2{}_\perp$-N_2 ligands move away from the cluster, see $Ni_3(\eta^2{}_\perp\text{-}N_2)_3(\mu^2{}_\perp\text{-}N_2)_3$ (Figure 4j), $Ni_3(\eta^2{}_\perp\text{-}N_2)_3(\mu_i\text{-}N_2)_3$, and $Ni_3(\eta^2{}_\perp\text{-}N_2)_3(\mu^2{}_i\text{-}N_2)_3$. On the other hand, $\eta^2{}_i$-N_2 ligands form mixed structures with bridge-bound ligands; they even stabilize the bonding of ligands in bridging positions, see $Ni_3(\eta^2{}_i\text{-}N_2)_3(\mu_i\text{-}N_2)_3$ and $Ni_3(\eta^2{}_i\text{-}N_2)_3(\mu^2{}_\perp\text{-}N_2)_3$ (Figure 4d,k).

Side-on bound ligands in the bridging position, $\mu^2{}_\perp$-N_2, have small binding energies. However, in some mixed structures, they are bound stronger to the cluster than η^2-N_2 ligands bound side-on to Ni atoms, see $Ni_3(\eta^2{}_\perp\text{-}N_2)_3(\mu^2{}_\perp\text{-}N_2)_3$ and $Ni_3(\eta^2{}_i\text{-}N_2)_3(\mu^2{}_\perp\text{-}N_2)_3$ (Figure 4j,k). Typical for all structures containing $\mu^2{}_\perp$-N_2 ligands is the substantial activation, both of the Ni_3 unit and the ligand molecules, with Δ(Ni−Ni) > 17 pm and Δ(N−N) = 6.6−9.6 pm in clusters with three and six ligands. $\mu^2{}_i$-type ligands are not bound in stable fashion. Their location does not permit other ligands to bind end-on. Thus, all studied structures with $\mu^2{}_i$-type ligands are unstable: $Ni_3(\mu^2{}_i\text{-}N_2)_3$ (Figure 2h), $Ni_3(\eta^2{}_i\text{-}N_2)_3(\mu^2{}_i\text{-}N_2)_3$, and $Ni_3(\eta_i\text{-}N_2)_3(\mu^2{}_i\text{-}N_2)_3$.

We were not able to identify a correlation between the BE per molecule and structure parameters, e.g. R(Ni−Ni) or R(Ni−N).

The obtained values of the average BE per N_2 ligand, more than 100 kJ/mol in several structures, suggest that the concept of N_2 as an "inert" probe ligand should be applied with due care;[39] even this typically inert molecule interacts notably with small (unsaturated) nickel clusters. In several structures studied, we note substantial geometric effects of the ligands enforcing this energy argument: (i) elongation of N−N bonds in most of the bridge-bound ligands and/or (ii) expansion of the Ni_3 moiety, especially in the presence μ_3 ligands, and (iii) decomposition of the clusters by larger numbers of N_2 ligands. The binding energy of the N_2 ligands also well exceeds the energy differences between various isomers of small Ni clusters.[16] However, dissociation of N_2 ligands after coordination is not observed in our model studies.

C. Ionization Potentials and Electron Affinities. The calculated vertical ionization potentials IP^0 and electron affinities EA^0 of the ligated clusters are larger than the corresponding values of bare Ni_3 (Table 3). This is an indication for strong back-donation of electron density from the Ni_3 unit to the ligands. There is no clear correlation between IP and EA values and the type of bonding of the N_2 ligands.

From the energy difference of optimized neutral, cationic, and anionic structures we calculated adiabatic values of the (first) ionization potential, IP^a, and the electron affinity, EA^a. The corresponding vertical and adiabatic quantities differ by up to 1.12 eV. As expected, one finds $IP^0 > IP^a$ and $EA^a > EA^0$ (Table 3).

The three stable planar structures of $Ni_3(N_2)_6$—$Ni_3(\eta_i\text{-}N_2)_3(\mu_i\text{-}N_2)_3$, $Ni_3(\eta^*_i\text{-}N_2)_6$, and $Ni_3(\eta^2{}_i\text{-}N_2)_3(\mu_i\text{-}N_2)_3$—have the largest IP^0 values, 7.58, 7.54, and 7.52 eV, respectively. The $Ni_3(N_2)_3$ complexes with bridge-bound ligands, $Ni_3(\mu_i\text{-}N_2)_3$, $Ni_3(\mu^2{}_\perp\text{-}N_2)_3$, and $Ni_3(\mu^2{}_i\text{-}N_2)_3$, have the smallest EA^0 values.

D. Comparison with Experiment and Other Theoretical Studies. For lack of experimental data on the bare cluster Ni_3, we checked the performance of the computational method for

Ni_2 where experimental values for bond length and dissociation energy are known. The experimental Ni−Ni bond length was reported at 220.0 pm[40] and 215.5 pm.[41] The corresponding experimental dissociation energy values of Ni_2 are 201 kJ/mol[40] and 198 kJ/mol,[41] i.e., the BE value per Ni atom is 100±1.0 kJ/mol. For both distance and energy, values mentioned in ref 41 are more recent. Our value for BE per atom, 142 kJ/mol, is larger than the experimental value; the optimized Ni−Ni distance, 214.9 pm, essentially agrees with the lower experimental value, 215.5 pm. However, calculated Ni−Ni distances of Ni_2 reported by other authors[17,30,42,43] for DF calculations, both at the local density and gradient corrected levels, are shorter, 199−213 pm, than the present result. Concomitantly, these calculations substantially overestimate the BE per atom; values from 161 to 304 kJ/mol have been reported.[17,30,42,43] This comparison for Ni_2 species suggests that our structural and energetic results for the bare cluster Ni_3 should be closer to those for the real cluster compared to other reported theoretical structures.

The triplet state of the bare cluster Ni_3, obtained in the present work in both D_{3h} and C_{2v} symmetry, agrees with previous theoretical investigations[17,20,30] that used various levels of DF calculations. Some LDA calculations,[20,43] however, found a singlet ground state. Our BP values of the Ni−Ni distance in Ni_3, 223−226 pm, compare well with distances, 223−224 pm, previously obtained with GGA methods (PW86[17] and BLYP[30]); LDA results ranged from 215 to 218 pm.[17,20,43] The BE per Ni atom of Ni_3, 175 kJ/mol, found here at the BP level, is smaller than the values calculated previously, both at the GGA,[17,30] 183−290 kJ/mol, and LDA levels, 231−357 kJ/mol.[17,20,43] As is often the case, LDA values of the BE are larger than calculated at the GGA level and concomitantly bond distances are shorter.[1,5,16,28]

Our calculated vertical and adiabatic IP (BP) values of the bare Ni_3 cluster, 6.48 and 6.29 eV, respectively, are 0.2−0.4 eV larger than experimental results of Knickelbein et al.,[44] 6.09 eV, and Watanabe,[45] 6.12−6.16 eV. The vertical IP value calculated by Reddy et al.,[30] 6.38 eV, obtained with the frozen-core GGA approach agrees with the present result, whereas the result of Pastor et al.,[46] IP = 6.2 eV, is closest to experiment, but was obtained with a tight-binding method without geometry optimization, using Ni−Ni distances fixed at the bulk nearest-neighbor value, 249.2 pm. ECP SCF-CI[47] and SCF-LCAO-MO/CI[48] calculations on the Ni_3 fragment, with the Ni−Ni distance fixed at the bulk nearest-neighbor distance, gave unrealistic results, 3.9 and 4.2 eV, respectively. The calculated vertical and adiabatic EA values of Ni_3, 1.05 and 1.28 eV, respectively, are also somewhat larger than experimental results,[49] 1.44 ± 0.06 eV.

The previous theoretical work of Reuse et al.[20] considered only a small number of structures of the complexes $Ni_3(N_2)_3$ and $Ni_3(N_2)_6$; they did not find the most stable structures reported here. Arranged in order of decreasing BE per ligand, they modeled three structures, $Ni_3(\eta_i\text{-}N_2)_3$, $Ni_3(\eta^2{}_i\text{-}N_2)_3$, and $Ni_3(\eta^2{}_\perp\text{-}N_2)_3$, of the complex with three ligands.[20] We also calculated a higher BE value per atom for the first structure, but for the other two we obtained very similar binding energies per BE values, 63 and 65 kJ/mol (Table 2). The only structure with six ligands reported in ref 20 is $Ni_3(\eta^*\text{-}N_2)_6$, according to the notation used here, which we found to be the second most stable among the $Ni_3(N_2)_6$ complexes. Because Reuse et al. used an LDA energy functional,[20] they obtained a BE per N_2 ligand of 248 and 200 kJ/mol for the most stable complexes with three and six ligands, respectively, which are more than twice as large as the present results, 116 and 98 kJ/mol (Table 2).

As mentioned above, we found that the values of the BE per ligand molecule of the most stable structures decrease with the number of coordinated N_2 ligands. However, the experimental results of Parks et al.[15] suggest the presence of only one Ni_3 complex with six coordinated N_2 ligand molecules. Experiments did not detect clusters with fewer N_2 ligands, possibly because the large IP values of the complexes complicate the investigations. To decrease the IP of the ligated cluster, some of the N_2 ligands were substituted by NH_3.[15] Based on the presence of peaks which correspond to the compounds $Ni_3(NH_3)(N_2)_5^+$ and $Ni_3(NH_3)_2(N_2)_4^+$, and the assumption that one NH_3 molecule substitutes one N_2 ligand, it was deduced "...that Ni_3 probably saturates with adsorption of six N_2 molecules".[15] This indirect evidence for the formation of $Ni_3(N_2)_6$ was obtained at saturation coverage and did not allow the detection of any complexes with fewer ligand molecules. Yet, both our calculations and previous theoretical studies[20] suggest that such complexes are rather stable. In fact, N_2 ligands of $Ni_3(N_2)_3$ on average are stronger bound than in $Ni_3(N_2)_6$ (Table 2). However, the total BE of the most stable cluster with six ligands is 140 kJ/mol larger than that of the cluster with three ligands; the cluster $Ni_3(N_2)_6$ is detected at saturation.

As our calculations show, the coordination of more than six N_2 molecules to Ni_3 leads to a considerable expansion or even the destruction of the metal cluster. Similar destruction processes were experimentally observed by Hintz and Ervin,[50,51] who investigated the chemisorption of N_2 and other molecules on nickel cluster anions. The destruction of Ni_3 at higher nitrogen pressure is likely the reason why Parks et al.[15] failed to detect experimentally Ni_3 complexes with more than six N_2 ligands.

To estimate which $Ni_3(N_2)_n$ complexes dominate in a reaction mixture of a given temperature where also decomposition into mononuclear species $Ni(N_2)_p$ may occur, we used a simple analysis based on energy changes calculated in this study (see Appendix). In that way, one can approximately simulate the product distribution resulting from the interaction of N_2 with Ni_3 clusters for varying values of the molecular ratio $k = [N_2]:[Ni_3]$ in the reaction mixture, which could be controlled in the experiment by the partial pressure of N_2. This analysis also permits one to follow how the number of ligands of Ni_3 complexes evolves and which mononuclear $Ni(N_2)_p$ species are formed with increasing partial N_2 pressure. For these calculations we used various energy results of our calculations: the BE of Ni atoms in the bare Ni_3 cluster (552 kJ/mol), the BE values of the most stable structures of each trinuclear complex $Ni_3(N_2)_n$ (Table 2), and the total BE of the mononuclear complexes $Ni(N_2)_p$, 156, 328, 399, and 440 kJ/mol for $p = 1-4$, respectively. Table 4 collects the energies of the various states of the system, relative to the reference, which comprises only bare Ni_3 moieties and N_2 in the gas phase. From these relative energies, we derived the corresponding product distribution in a canonical ensemble of molar ratio k at the experimental temperature[15] of −80 °C (see the Appendix for details). As can be seen from Figure 8, at molar ratios near 3, 4, 5, 6, and 7, the corresponding most stable complexes $Ni_3(N_2)_n$, $n = 3-7$, should be dominant. The most stable complex with six ligands is a special case as it exists at molar rations between 4.5 and 8.0 and dominates in a larger interval of molar ratios than the other complexes. For molar ratios k larger than 7, complexes of Ni_3 with more than seven ligands are unlikely to be formed due to the fact that decomposition into mononuclear $Ni(N_2)_p$ species is preferred; $Ni(N_2)_3$

TABLE 4: Calculated Relative Energies of Formation, $E_1(n)$[a] and $E_2(p)$,[b] of Tri- and Mononuclear Complexes $Ni_3(N_2)_n$ and $Ni(N_2)_p$, Respectively, for Molar Ratios $k = 3-12$

	$E_1(n)$ for $n =$							$E_1(p)$ for $p =$			
k	3	4	5	6	7	8	9	1	2	3	4
3	116.0	107.0	101.8	98.0	87.3	73.1	72.0	−19.0	76.5	74.7	66.3
4	87.0	107.0	101.8	98.0	87.3	73.1	72.0	−14.3	76.5	74.7	66.3
5	69.6	85.6	101.8	98.0	87.3	73.1	72.0	−11.4	76.5	74.7	66.3
6	58.0	71.3	84.8	98.0	87.3	73.1	72.0	−9.5	76.5	74.7	66.3
7	49.7	61.1	72.7	84.0	87.3	73.1	72.0	−8.1	65.6	74.7	66.3
8	43.5	53.5	63.6	73.5	76.4	73.1	72.0	−7.1	57.4	74.7	66.3
9	38.7	47.6	56.6	65.3	67.9	65.0	72.0	−6.3	51.0	74.7	66.3
10	34.8	42.8	50.9	58.8	61.1	58.5	64.8	−5.7	45.9	67.2	66.3
11	31.6	38.9	46.3	53.5	55.5	53.2	58.9	−5.2	41.7	61.1	66.3
12	29.0	35.7	42.4	49.0	50.9	48.8	54.0	−4.8	38.3	56.0	66.3
BE_{total}[c]	348	428	509	588	611	585	648	156	328	399	440

[a] Equations 1′ and 2′; values of opposite sign are shown. [b] Equations 3′ and 4′; values of opposite sign are shown. [c] Total BE of tri- or mononuclear complexes (in kJ/mol); $BE_{total}(Ni_3) = 525$ kJ/mol.

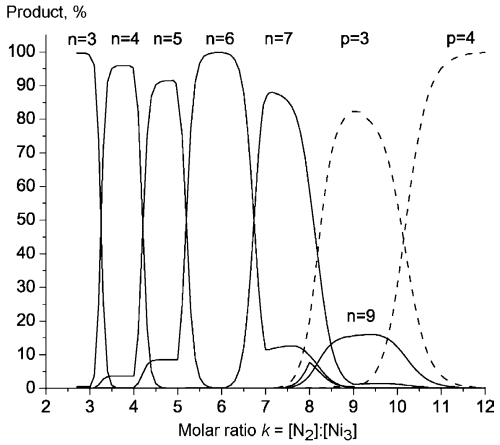

Figure 8. Simulated equilibrium product distribution in a reaction mixture of molar ratio $k = [N_2]:[Ni_3]$ at temperature −80 °C [ref 15], based on calculated ligand binding energies. Relative concentrations of trinuclear and mononuclear complexes are shown as solid $[Ni_3(N_2)_n]$ and dashed $[Ni(N_2)_p]$ lines, respectively.

species are the majority for $k = 9$, whereas $Ni(N_2)_4$ species are formed for even larger values of the molar ratio $k = [N_2]:[Ni_3]$.

In the derivation of the product distribution described above, we assumed equilibrium conditions in the reaction mixture consisting only of bare Ni_3 clusters, N_2 molecules in the gas phase as reagents, as well as tri- and mononuclear complexes $Ni_3(N_2)_n$ and $Ni(N_2)_p$, respectively, as products. Unfortunately, the experimental conditions in ref 15 are much more complicated due to the presence of various bare Ni_x clusters. In that sense, the exact molar ratio $k = [N_2]:[Ni_3]$ is not known. The lack of complexes with seven N_2 ligands in the experiment or, viewed differently, the discrepancy between the results of the experiments and the present modeling of the product distribution could be due to several factors: e.g. (i) simplifying assumptions of the model for deriving the product distribution; (ii) uncertainties in the BE values obtained in our DF calculations due to imposed symmetry restrictions; and (iii) the indirect method for determining the number of N_2 ligands coordinated to a Ni_3 cluster in the experiment (see the above description of the experiment). For instance, if the difference of the average BE values per ligand between $Ni_3(N_2)_6$ and $Ni_3(N_2)_7$ would be calculated at about 6 kJ/mol larger, than complexes with six N_2 ligands would also dominate for molar ratios $k = 7-8$ whereas the dominance of mononuclear complexes for larger values of k would remain.

The species produced by the decomposition of $Ni_3(N_2)_n$, e.g. complexes $Ni(N_2)_3$ and $Ni(N_2)_4$, were not detected in the experiment of Parks et al.[15] because the mass spectrum was recorded only for larger mass/charge ratios. The mononuclear complexes $Ni(N_2)_p$ ($p = 1-4$) were obtained experimentally by condensation of Ni atoms with N_2 at 4.2−10 K and were identified by matrix isolation followed by IR and Raman spectroscopy.[52] Previous experimental and theoretical studies[36,53] showed similar structures as those found in our calculations.

V. Conclusions

We studied structures of complexes of a Ni_3 cluster with three to nine N_2 ligands, imposing relevant symmetry constraints, with a density functional method. The BE per ligand molecule was calculated to decrease when the number of coordinated N_2 molecules in the complexes increased, even though the total BE of the complexes increased up to seven ligands. The calculations suggest that Ni_3 clusters with more than seven ligands are unstable against decomposition into mononuclear species. In a canonical ensemble, simulations of the distribution of mono- and trinuclear complexes showed that complexes with three, four, six, and seven ligands dominated for increasing values of the molar ratio $k = [N_2]:[Ni_3]$. The complex $Ni_3(N_2)_6$ was among the dominant trinuclear species at saturation, in agreement with the experiment. However, according to the simulations, complexes with seven ligands, not observed in the experiment, should also occur to a noticeable degree at intermediate values of the molar ratio. This partial discrepancy likely originates from difficulties to simulate precisely the product distribution at molar ratios $k \approx 7$, where the $Ni_3(N_2)_7$ species are expected to dominate; an alternative reason could be that in experiment the dominant species is determined in an indirect way that involves not only N_2, but also ammonia as a ligand. At molar ratios $k = [N_2]:[Ni_3]$ equal or larger than 8, mononuclear $Ni(N_2)_p$ complexes ($p = 3-4$) are predicted to dominate. To achieve a more complete picture of how N_2 ligands interact with nickel clusters with three or more metal atoms, new experiments are desirable; they should search the full range of molar ratios including also mono- and binuclear complexes at higher molar ratios. Such quasiequilibrium experiments would allow a closer comparison with the results of the present (and future) computational studies.

Although N_2 molecules often are assumed to be inert ligands, their interaction with a Ni_3 cluster was calculated to be quite strong, above 100 kJ/mol BE per ligand for the most stable structures. There are various experimental studies on complexes with N_2 ligands, but most of them provide only spectral or structural information, confirming the coordination of the N_2 molecule to a metal center (atom or cation).[52−54] Complementary computational studies[55] estimated the BE of N_2 ligands in such

complexes, from very weak bonding at alkaline cations or cationic silver clusters with BE values up to 30 kJ/mol[55] to stronger bonding at transition metal cations or atoms with BE values of more than 100 kJ/mol,[53] comparable to the present results.

The most stable type of bonding of N_2 molecules to a Ni_3 cluster is end-on at a Ni atom, η, or to a Ni−Ni bond, μ; side-on bonding, η^2, to a Ni atom is the next weaker coordination mode. Bonding in a 3-fold position above the Ni_3 moiety, μ_3, depends strongly on the other type of ligands in the complex. For stable bridge-bonded ligands, μ_i and $\mu_\perp$, we calculated a larger elongation of the N−N bonds. As a trend, the most stable types of bonding to a Ni atom, end-on η^*_i, η_i, and η_t, exhibit the least elongation of N−N bonds (1.3−2.1 pm), whereas the other types of bonding, η^2 and μ-types, are accompanied by larger N−N elongation values, ∼3−9 pm. All end-on bound ligands are polarized, most strongly when the N_2 ligand is in the μ_i and μ_3 positions.

The binding energy per ligand for a given structure in general decreases from the anionic to the neutral and the cationic forms of the complex. For most model structures studied, the geometry of the complex does not vary much with the charge, although there are several exceptions where the structures of neutral and ionic forms of the complex differ substantially (Table 1). As a rough trend, the activation of the N−N bond of the ligands is larger for anionic and smaller in cationic complexes.

The metal−ligand charge separation is smaller for linearly bound η-N_2 ligands, where the Ni_3 moiety carries a positive charge of only 0.12−0.18 e. The positive charge of the metal unit increases for side-on η ligands (up to 0.39 e) and, more strongly, for complexes with μ ligands, up to 1.21 e for $\mu^2_\perp$ coordination. Complexes with all types of η ligands have larger Ni 4s populations compared to complexes with μ or mixed types of ligands. As a trend, the Ni 4s population decreases and the Ni 4p population increases with increasing number of N_2 ligands. Coordination of N_2 leads to a quenching of the triplet state of the bare Ni_3 cluster, similar to the reduction of the paramagnetism of transition metal clusters due to CO adsorption.[3,6,56] In addition, coordination of N_2 ligands increases the vertical and adiabatic ionization potentials and electron affinities.

Acknowledgment. We thank S. Krüger and K. M. Neyman for helpful discussions. This work was supported by the National Science Fund (Bulgaria), Deutsche Forschungsgemeinschaft, Alexander von Humboldt Foundation (through an equipment donation and the institute cooperation program), and Fonds der Chemischen Industrie (Germany).

Supporting Information Available: Tables of coordinates of the atoms in the optimized neutral structures of the ligated clusters shown in Figures 2−6 and corresponding cationic and anionic complexes. This material is available free of charge via the Internet at http://pubs.acs.org.

Appendix: Simulating the Distribution of Product Complexes $Ni_3(N_2)_n$ and $Ni(N_2)_p$ Obtained after Coordination of N_2 Ligands to Ni_3 Clusters

To discuss the distribution of complexes after coordinating N_2 ligands to a Ni_3 moiety, we assume a canonical ensemble at temperature $T = 193$ K as used in the experiment.[15] As stated, we consider trinuclear complexes $Ni_3(N_2)_n$ ($n = 3-9$) and mononuclear complexes $Ni(N_2)_p$ ($p = 1-4$) formed after decomposition of Ni_3 moieties; in this approximation, we neglect the possible formation of binuclear complexes. Using the calculated BE values for N_2 ligands in the mononuclear and the most stable isomers of the trinuclear complexes, we assign energies to the various states which are defined by a fixed molar ratio $k = [N_2]:[Ni_3]$.

Specifically, we consider a situation with starting concentrations $[Ni_3] = 1$ mol/volume and $[N_2] = k$ mol/volume and write down the concentrations when only a single reaction to one of the complexes $Ni_3(N_2)_n$ or $Ni(N_2)_p$ has run to completion. Then the final concentrations of the trinuclear complexes would be

$$[Ni_3(N_2)_n] + (k - n)[N_2] \quad \text{if } k > n, \text{ i.e. for an excess of } N_2 \quad (1)$$

$$(k/n)[Ni_3(N_2)_n] + (k - k/n)[Ni_3] \quad \text{otherwise} \quad (2)$$

The corresponding energy changes per mole of N_2 (either bound in a complex or free) are

$$E_1(n) = -BE_{total}\{Ni_3(N_2)_n\}/k \quad \text{if } k \geq n \quad (1')$$

$$E_1(n) = -BE_{total}\{Ni_3(N_2)_n\}/n \quad \text{if } k \leq n \quad (2')$$

where BE_{total} is the total binding energy of the complex $Ni_3(N_2)_n$. Similarly, we obtain for the final concentrations of the mononuclear complexes:

$$3[Ni(N_2)_p] + (k - 3p)[N_2] \quad \text{if } k > 3p, \text{ i.e. for an excess of } N_2 \quad (3)$$

$$(k/p)[Ni(N_2)_p] + (1 - k/3p)[Ni_3] \quad \text{otherwise} \quad (4)$$

The corresponding energy changes per mole of N_2 are

$$E_2(p) = -[3BE_{total}\{Ni(N_2)_p\} - BE_{total}\{Ni_3\}]/k \quad \text{if } k \geq 3p \quad (3')$$

$$E_2(p) = -[3BE_{total}\{Ni(N_2)_p\} - BE_{total}\{Ni_3\}]/3p \quad \text{if } k \leq 3p \quad (4')$$

The resulting energies $E_1(n)$ for $n = 3-9$ and $E_2(p)$ for $p = 1-4$, based on the results of the present DF calculations, are collected in Table 4.

Then, at equilibrium, the product distribution in a reaction mixture at fixed molar ratio $k = [N_2]:[Ni_3]$ is governed by the relative Boltzmann factors $\exp[-E_i(m)/RT]$, where $E_i(m)$ is the relative energy $E_1(n)$ or $E_2(p)$, respectively, according to eqs 1′−4′. The resulting product distribution for $T = 193$ K is shown in Figure 8.

References and Notes

(1) Pacchioni, G.; Krüger, S.; Rösch, N. In *Metal Clusters in Chemistry*; Braunstein, P., Oro, L. A., Raithby, P. R., Eds.; Wiley−VCH: Weinheim, Germany, 1999; p 1392.
(2) Kaldor, A.; Cox, D. M.; Zakin M. R. *Adv. Chem. Phys.* **1988**, *70*, 211.
(3) Pacchioni, G.; Rösch, N. *Acc. Chem. Res.* **1995**, *28*, 390.
(4) Rosen, A. *Adv. Quantum Chem.* **1998**, *30*, 235.
(5) Alonso, J. A. *Chem. Rev.* **2000**, *100*, 637.
(6) (a) Rösch, N.; Pacchioni, G. *Inorg. Chem.* **1990**, *29*, 2901. (b) Rösch, N.; Ackermann, L.; Pacchioni, G. *J. Am. Chem. Soc.* **1992**, *114*, 3549. (c) Rösch, N.; Ackermann, L.; Pacchioni, G. *Chem. Phys. Lett.* **1992**, *199*, 275. (d) Pacchioni, G.; Ackermann, L.; Rösch, N. *Gazz. Chem. Ital.* **1992**, *122*, 205. (e) Rösch, N.; Ackermann, L.; Pacchioni, G. *Inorg. Chem.* **1993**, *32*, 2963. (f) Pacchioni, G.; Chung, S.-C.; Krüger, S.; Rösch, N. *Chem. Phys.* **1994**, *184*, 125. (g) Matveev, A. V.; Neyman, K. M.; Pacchioni, G.; Rösch, N. *Chem. Phys. Lett.* **1999**, *299*, 603. (h) Krüger, S.; Seemüller, T. J.; Wörndle, A.; Rösch, N. *Int. J. Quantum Chem.* **2000**, *80*, 567.
(7) Sakurai, M.; Watanabe, K.; Sumiyama, K.; Suzuki, K. *J. Chem. Phys.* **1999**, *111*, 235.

(8) Meloni, G.; Schmude, R. W.; Kingcade, J. E., Jr.; Gingerich, K. A., Jr. *J. Chem. Phys.* **2000**, *113*, 1852.

(9) Kaldor, A.; Cox, D. M. *J. Chem. Soc., Faraday Trans.* **1990**, *86*, 2459.

(10) Cox, D. M.; Fayet, P.; Brickman, R.; Hahn, M. Y.; Kaldor, A. *Catal. Lett.* **1990**, *4*, 271.

(11) Knickelbein, M. B. *Annu. Rev. Chem.* **1999**, *50*, 79.

(12) Holmgren, L.; Rosen, A. *J. Chem. Phys.* **1999**, *110*, 2629. Holmgren, L.; Anderson, M.; Rosen A. *J. Chem. Phys.* **1998**, *109*, 3232.

(13) Amentrout, P. B. *Annu. Rev. Phys. Chem.* **2001**, *52*, 423.

(14) (a) Parks, E. K.; Klots, T. D.; Winter, B. J.; Riley, S. J. *J. Chem. Phys.* **1994**, *99*, 5831. (b) Ho, J.; Parks, E. K.; Zhu, L.; Riley, S. J. *Chem. Phys.* **1995**, *201*, 245. (c) Parks, E. K.; Zhu, L.; Ho, J.; Riley, S. J. *J. Chem. Phys.* **1995**, *102*, 7377. (d) Parks, E. K.; Nieman, G. C.; Kerns, K. P.; Riley, S. J. *J. Chem. Phys.* **1998**, *108*, 3731. (e) Parks, E. K.; Kerns, K. P.; Riley, S. J. *J. Chem. Phys.* **2000**, *112*, 3384.

(15) Parks, E. K.; Zhu, L.; Ho, J.; Riley, S. J. *J. Chem. Phys.* **1994**, *100*, 7206.

(16) Krüger, S.; Seemüller, T. J.; Wörndle, A.; Rösch, N. *J. Quantum Chem.* **2000**, *80*, 567.

(17) Castro, M.; Jamorski, C.; Salahub, D. R. *Chem. Phys. Lett.* **1997**, *271*, 133.

(18) Chien, C.-H.; Blaisten-Barojas, E.; Pederson, M. R. *Phys. Rev. A* **1998**, *58*, 2196.

(19) van Leeuwen, D. A.; van Ruitenbeek, J. M.; de Jongh, L. J.; Ceriotti, A.; Pacchioni, G.; Longoni, G.; Häberlen, O. D.; Rösch, N. *Phys. Rev. Lett.* **1994**, *73*, 1432.

(20) Reuse, F. A.; Khanna, S. N.; Reddy, B. V.; Buttet, J. *Chem. Phys. Lett.* **1997**, *267*, 258.

(21) (a) Becke, A. D. *Phys. Rev. A* **1988**, *38*, 3098. (b) Perdew, J. P. *Phys. Rev. B* **1986**, *33*, 8822. Perdew, J. P. *Phys. Rev. B* **1986**, *34*, 7406.

(22) Dunlap, B. I.; Rösch, N. *Adv. Quantum Chem.* **1990**, *21*, 317.

(23) Belling, T.; Grauschopf, T.; Krüger, S.; Mayer, M.; Nörtemann, F.; Staufer, M.; Zenger, C.; Rösch, N. In *High Performance Scientific and Engineering Computing*; Lecture Notes in Computational Science and Engineering, Vol. 8; Bungartz, H.-J., Durst, F., Zenger, C., Eds.; Springer: Heidelberg, Germany, 1999; p 439.

(24) Belling, T.; Grauschopf, T.; Krüger, S.; Nörtemann, F.; Staufer, M.; Mayer, M.; Nasluzov, V. A.; Birkenheuer, U.; Hu, A.; Matveev, A. V.; Shor, A. M.; Fuchs-Rohr, M. S. K.; Neyman, K. M.; Ganyushin, D. I.; Kerdcharoen, T.; Woiterski, A.; Rösch, N. *ParaGauss*, Version 2.2; Technische Universität München: München, Germany, 2001.

(25) Nasluzov, V. A.; Rösch, N. *Chem. Phys.* **1996**, *210*, 413.

(26) (a) Wachters, A. J. H. *IBM Tech Rep RJ584 1969*. (b) Wachters, A. J. H. *Chem. Phys.* **1970**, *52*, 1033. (c) Van Duijneveldt, F. B. *IBM Res. Rep. RJ* **1971**, 945.

(27) *Handbook of Chemistry and Physics*, 62nd ed.; CRC press, Boca Raton, FL, 1981−1982; p F177.

(28) Görling, A.; Trickey, S. B.; Gisdakis, P.; Rösch, N. In *Topics in Organometallic Chemistry*; Brown, J., Hofmann, P., Eds.; Springer: Heidelberg, Germany, 1999; Vol. 4, p 109.

(29) Zhang, Y.; Yang, W. *J. Chem. Phys.* **1998**, *109*, 2604.

(30) Reddy, B. V.; Nayak, S. K.; Khanna, S. N.; Rao, B. K.; Jena, P. *J. Phys. Chem. A* **1998**, *102*, 1748.

(31) The BE per Ni atom is calculated with respect to three separated Ni atoms in the electronic configuration $3d^94s^1$.

(32) With our choice of axes, the irreproducible representations correspond to each other as follows ($D_{3h} \rightarrow C_{2v}$): $a_1' \rightarrow a_1$, $a_2' \rightarrow b_2$, $e' \rightarrow a_1 + b_2$, $a_1'' \rightarrow a_2$, $a_2'' \rightarrow b_1$, $e'' \rightarrow a_2 + b_1$.

(33) We checked three different electronic configurations in C_{2v} symmetry, which could correspond to the second configuration in D_{3h}. Only one of these configurations converged, namely when one electron was distributed equally over the two essentially degenerate orbitals, a_1 and b_2, which derive from the orbital e′ of D_{3h}; the corresponding configuration is $(a_1)^{35.5}(a_2)^{10}(b_1)^{14}(b_2)^{24.5}$. The resulting energy is the same as in the other structure of C_{2v} symmetry (see ref 32) and the R(Ni−Ni) distances are 225.6 and 225.5 pm.

(34) Vertical IE and EA values for Ni_3 in C_{2v} symmetry are not reported because the SCF procedures did not converge for the corresponding anionic and cationic structures.

(35) Due to the enforced spatial symmetry, the electron density is equally distributed on symmetry-equivalent parts of a system, even if separated in space. Thus, one should emphasize the model character of these calculations which excluded symmetry breaking that might occur in open-shell systems; see ref 29.

(36) Timney, J. A. *Spectrochim. Acta* **1995**, *51A*, 33.

(37) Jorgensen, W. L.; Salem, L. *The Organic Chemist's Book of Orbitals*; Academic Press: New York, 1973.

(38) (a) King, D. A. *Surf. Sci.* **1968**, *9*, 375. (b) Grunze, M.; Driscoll, R. K.; Burland, G. N.; Gomish, J. C. L.; Pritchard, J. *Surf. Sci.* **1979**, *89*, 381.

(39) One may consider a probe molecule inert when its binding to the substrate is weak and induces only minor changes of intraunit distances, i.e., inside the cluster and the probe.

(40) Morse, M. O.; Hansen, G. P.; Langridge-Smith, P. R. R.; Zheng, L. S.; Geusic, M. E.; Michalopoulos, D. L.; Smalley. R. E. *J. Chem. Phys.* **1984**, *80*, 5400.

(41) Pinegar, J. C.; Langenberg, J. D.; Arrington, C. A.; Spain, E. M.; Morse, M. D. *J. Chem. Phys.* **1995**, *102*, 666.

(42) Gutsev, G. L.; Bauschlicher, C. W., Jr. *J. Phys. Chem. A* **2003**, *107*, 4755.

(43) Reuse, F. A.; Khanna, S. N. *Chem. Phys. Lett.* **1995**, *234*, 77.

(44) Knickelbein, M. B.; Yang, S.; Riley, S. *J. Chem. Phys.* **1990**, *93*, 94.

(45) Watanabe, K. *J. Chem. Phys.* **1954**, *22*, 1564.

(46) Pastor, G. M.; Dorantes-Davila, J.; Bennemann, K. H. *Chem. Phys. Lett.* **1988**, *148*, 459.

(47) Basch, H.; Newton, M. D.; Moskowitz, J. W. *J. Chem. Phys.* **1980**, *73*, 4492.

(48) Tomanari, M.; Tatewaki, H.; Nakamura, T. *J. Chem. Phys.* **1986**, *85*, 2975.

(49) Liu, S.-R.; Zhai, H.-J.; Wang, L.-S. *J. Chem. Phys.* **2002**, *117*, 9758.

(50) Hintz, P. A.; Ervin, K. M. *J. Chem. Phys.* **1995**, *103*, 7897.

(51) At variance with the domination of $Ni_3(N_2)_6$ complexes in the case of neutral Ni_3 clusters,[15] Hintz and Ervin[50] observed at most three N_2 ligands coordinated to Ni_3^- clusters.

(52) (a) Burdett, J. K.; Turner, J. J. *Chem. Commun.* **1971**, 885. (b) Huber, H.; Kundig, E. P.; Moskovits, M.; Ozin, G. A. *J. Am. Chem. Soc.* **1973**, *95*, 332. (c) Klatzbucher, W.; Ozin, G. A. *J. Am. Chem. Soc.* **1975**, *97*, 2672.

(53) (a) Andrews, L.; Citra, A.; Chertihin, G. V.; Bare, W. D.; Neurock, M. *J. Phys. Chem. A* **1998**, *102*, 2561. (b) Chen, M.; Zhon, M.; Zhang, L.; Qin, Q. *J. Phys. Chem. A* **2000**, *104*, 8627.

(54) (a) Allen, A. D.; Senoff, C. V. *Chem. Commun.* **1965**, 621. (b) Miessner, H. *J. Am. Chem. Soc.* **1994**, *116*, 11522. (c) Hadjiivanov, K.; Ivanova, E.; Klisurski, D. *Catal. Lett.* **2001**, *70*, 75.

(55) (a) Schooss, D.; Gilb, S.; Kaller, J.; Kappes, M. M.; Furche, F.; Köhn, A.; May, K.; Ahlrichs, R. *J. Chem. Phys.* **2000**, *113*, 5361. (b) Vayssilov, G. N.; Hu, A.; Birkenheuer, U.; Rösch, N. *J. Mol. Catal. A* **2000**, *162*, 135.

(56) Mineva, T.; Russo, N.; Freund, H.-J. *J. Phys. Chem. A* **2001**, *105*, 10723.